Base-pairing requirements for small RNA-mediated gene silencing of recessive self-incompatibility alleles in *Arabidopsis halleri.*

N. Burghgraeve[1], S. Simon[1], S. Barral[1], I. Fobis-Loisy[2], A-C Holl[1], C. Poniztki[1], E. Schmitt[1], X. Vekemans[1], V. Castric[1*]

1. CNRS, Univ. Lille, UMR 8198 - Evo-Eco-Paleo, F-59000 Lille, France
2. Laboratoire Reproduction et Développement des Plantes, Univ de Lyon, ENS de Lyon, UCB Lyon1, CNRS, INRA, F-69342, Lyon, France

* Corresponding author

E-mail : Vincent.Castric@univ-lille.fr

Abstract

Small RNAs (sRNA) are central regulators of gene expression, yet identifying the molecular alphabet of sRNA-target interactions remains challenging. Here, we take advantage of the dominance hierarchy among self-incompatibility alleles in *Arabidopsis halleri* to evaluate the base-pairing requirements for effective transcriptional silencing by a highly diversified set of sRNA-target interactions. We used RT-qPCR to follow temporal expression of the pollen (*SCR*) and pistil (*SRK*) determinants of self-incompatibility in numerous heterozygous combinations. *SCR* and *SRK* had sharply distinct expression dynamics through flower development. Recessive *SCR* alleles were transcriptionally silenced in all heterozygote combinations examined, bringing levels of *SCR* transcripts below detection limits regardless of the position of the sRNA target along the *SCR* sequence. A simple threshold model of base-pairing for the sRNA-target interaction captures most of the variation in *SCR* transcript levels. In contrast, both *SRK* alleles were expressed at similar levels in all heterozygote genotypes. We show that the base-pairing requirements for effective transcriptional silencing by these sRNAs are broadly similar to those of canonical microRNAs, even though they are believed to function in sharply different ways. We discuss the implications for the evolutionary processes associated with the

origin and maintenance of the dominance hierarchy among self-incompatibility alleles.

Author summary

Small non-coding RNAs are important regulatory molecules that achieve their function through sequence similarity with their target sites. In many cases however, the precise base-pairing requirements for effective regulation are poorly known. At the self-incompatibility (SI) locus in Arabidopsis, dominance between alleles is pervasive and is controlled in pollen by small non-coding RNAs produced by dominant alleles that target specific sequence motifs on recessive alleles. Here we use a large number of heterozygote combinations of SI alleles to show that dominance is tightly associated with strong transcriptional silencing of the recessive alleles in presence of a more dominant allele. We take advantage of this highly diversified system of multiple sRNAs and their diversified target sites to determine the base-pairing requirements for successful small-RNA mediated transcriptional silencing. The threshold model that we identify has important functional and evolutionary implications for this complex regulatory mechanism.

Introduction

Small non-coding RNAs are short RNA molecules (20-25nt) with a range of regulatory functions whose central importance has constituted a major discovery in the last 20 years (Vazquez *et al.*, 2010; Aalto & Pasquinelli, 2012). The best-known members of this class of molecules are microRNAs, which are typically involved in post-transcriptional gene silencing and regulate the activity of their target gene in *trans* by either mRNA cleavage (quickly followed by degradation) or by blocking translation (Li *et al.*, 2014). In some cases, the action of microRNAs leads to the production of secondary phased short interfering RNAs (pha-siRNAs) by their target coding or non-coding sequence, which in turn can regulate downstream targets (Fei *et al.*, 2013). Another major set of small RNAs is heterochromatic short interfering RNAs (hc-siRNAs) which are mediating transcriptional silencing of repeat sequences in the genome through epigenetic modification by the RNA-dependent DNA methylation pathway (RdDM, Matzke *et al.*, 2009).

Both microRNAs and siRNAs guide their effector molecules (members of the ARGONAUTE gene family: AGO1 and AGO4, respectively) to their target sites by sequence similarity through base-pairing. For plant microRNAs, sequence similarity with the target sequence is typically very high and appears to be a shared

feature of all functionally verified interactions (Wang *et al.*, 2015). Total base-pairing complementarity, however, is not the sole determinant of target specificity, and the position of the mismatches along the microRNA:target duplex is also important. Indeed, expression assays showed that while individual mismatches typically have limited functional consequences, they can also entirely inactivate the interaction when they hit specific positions such as e.g. the 10^{th} and 11^{th} nucleotide, corresponding to the site of cleavage (Jones-Rhoades *et al.*, 2006). Furthermore, the position of mismatches along the microRNA:target duplex also seems to be crucial, with a greater tolerance in the 3' than the 5' region of the microRNA (up to four mismatches generally have limited functional consequences in the 3' region, while only two mismatches in the 5' region seem sufficient to abolish the target recognition capability; Liu *et al.*, 2014, Mallory *et al.*, 2004; Parizotto *et al.*, 2004; Schwab *et al.*, 2005). These observations have led to the formulation of general "rules" for microRNA targeting (Axtell & Meyers, 2018), but in the same time they also revealed a large number of exceptions. As a result, *in silico* prediction of microRNA target sites currently remains a difficult challenge (Ding *et al.*, 2012; Axtell & Meyers, 2018). For other types of small RNAs (pha-siRNAs and hc-siRNAs), even less is known about the base-pairing requirements for targeting, mostly

because of the absence of experimentally confirmed examples of discrete, single siRNA target sites either in *cis* or in *trans* (Wang *et al.*, 2015).

In this context, the recent discovery by Tarutani *et al.* (2010), Durand *et al.* (2014) and Yasuda *et al.*, (2016) of a highly diversified set of small non-coding RNAs at the gene cluster controlling self-incompatibility (SI) in Brassicaceae, provides an experimentally tractable model to evaluate the base-pairing requirements for silencing by a set of sRNAs that are regulating expression of a single gene. Sporophytic SI is a genetic system that evolved in several hermaphroditic plant lineages to enforce outcrossing by preventing self-fertilization, hence avoiding inbreeding depression (De Nettancourt, 2001). In the Brassicaceae family, SI is controlled by a single genomic region called the "S-locus", which contains two tightly linked genes, namely *SCR* and *SRK,* that encode the pollen S-locus cysteine-rich and the stigma S-locus receptor kinase recognition proteins, respectively. This system involves a polymorphism in which multiple deeply diverged allelic lines are maintained, and accordingly a large number of S-alleles is typically found in natural populations of self-incompatible species (Castric & Vekemans, 2004). With such a large allelic diversity and the very process of self-rejection, most individual plants are heterozygotes at the S-locus. Yet in most

cases, only one of the two S-alleles in a heterozygous genotype is expressed at the phenotypic level in either pollen or pistil, as can be revealed by controlled pollination assays on pollen or pistil tester lines (Llaurens *et al.*, 2008; Durand *et al.*, 2014). Which of the two alleles is expressed is determined by their relative position along a dominance hierarchy, whose molecular basis for the pollen phenotype has been initially studied in the genus Brassica. In this genus, dominance is controlled at the transcriptional level in pollen (Schopfer 1999, Kakizaki et al. 2003). Transcriptional silencing of recessive alleles by dominant alleles is caused by 24nt-long trans-acting small RNAs produced by dominant S-alleles and capable of targeting a DNA sequence in the promoter sequence of the *SCR* gene of recessive S-alleles, provoking DNA methylation (Shiba et al. 2006). Details of how these sRNAs achieve their silencing function remains incompletely understood (Finnegan *et al.*, 2011), but it is clear that their biogenesis is similar to that of microRNAs (*i.e.,* they are produced by a short hairpin structure), while their mode of action is rather reminiscent of that of siRNAs (*i.e.,* the transcriptional gene silencing functions through recruitment of the methylation machinery). Strikingly, the full dominance hierarchy in the Brassica genus seems to be controlled by just two small RNAs called *Smi* and *Smi2* (Tarutani *et al.*, 2010, Yasuda *et al.* 2016). *Smi* and *Smi2* target distinct DNA sequences, but both are

154 located in the promoter region of *SCR*, and both seem to involve
155 DNA methylation and 24-nt active RNA molecules.

156 The dominance hierarchy in Brassica is however peculiar in that
157 only two ancestral allelic lineages segregate in that genus (the class
158 I and class II alleles referred to above, see *e.g.* Leducq *et al.*,
159 2014), whereas self-incompatible species in Brassicaceae typically
160 retain dozens of highly divergent ancestral allelic lineages (Castric
161 & Vekemans, 2004). A recent study showed that in *Arabidopsis*
162 *halleri*, a Brassicaceae species with multiple allelic lineages at the
163 S-locus, the dominance hierarchy among S-alleles in pollen is
164 controlled by not just two but as many as eight different sRNA
165 precursor families and their target sites, whose interactions
166 collectively determine the position of the alleles along the
167 hierarchy (Durand *et al.*, 2014). In that genus, much less is known
168 about the mechanisms by which the predicted sRNA-target
169 interactions translate into the dominance phenotypes. First, the
170 expression dynamics of the *SCR* gene across flower development
171 stages is poorly known. Indeed, Kusaba et al. (2002) measured
172 expression of *SCR* alleles in *A. lyrata,* but focused on only two S-
173 alleles (*SCRa* and *SCRb*, also known as *AlSCR13* and *AlSCR20*,
174 respectively, in Mable et al. 2003) and showed striking differences
175 in their expression dynamics in anthers. Hence, the developmental
176 stage at which the transcriptional control of dominance in pollen

177 should be tested is not clear. Second, while they did confirm
178 monoallelic expression, consistent with the observed dominance
179 relationship between the two alleles (*SCR*b > *SCR*a, Kusaba et al.
180 2002), the fact that only a single heterozygote combination was
181 measured among the myriad possible combinations given the large
182 number of S-alleles segregating in that species (at least 38 S-
183 alleles: Castric *et al.*, 2008) prevents generalization at this step.
184 Hence, a proper experimental validation of the transcriptional
185 control of dominance in Arabidopsis is still lacking. Third, Durand
186 *et al.*, (2014) observed rare sRNA-target interaction predictions
187 that did not agree with the observed dominance phenotype. In
188 particular, they identified cases where no sRNA observed as being
189 produced by a dominant allele was predicted to target the *SCR*
190 gene of a recessive allele, while the dominance phenotype had
191 been well established phenotypically by controlled crosses (*e.g.*
192 Ah04>Ah03) suggesting the possibility that mechanisms other than
193 transcriptional control may be acting. Conversely, in other rare
194 cases, sRNAs produced by a recessive S-allele were predicted to
195 target the *SCR* gene of a more dominant allele, suggesting
196 exceptions to the set of base-pairing rules used to predict target
197 sites. Fourth, although the target sites for the two sRNAs in
198 Brassica were both located in the promoter sequence, and can thus
199 be reasonably expected to prevent transcriptional initiation through

local modification of the chromatin structure associated with DNA methylation, many of the predicted sRNA target sites in *A. halleri* are rather mapped to the *SCR* intron or the intron-exon boundary (beside some in the promoter as well), which suggests that distinct silencing pathways might be acting (Cuerda-Gil & Slotkin, 2016). It thus remains to be determined whether transcriptional control is also valid when the targets are at other locations along the *SCR* gene structure. Finally, the dominance hierarchy at the female determinant *SRK* differs from that at *SCR*, co-dominance being more frequent than on the pollen side both in Brassica (Hatakeyama *et al.*, 2001) and in *A. halleri* (Llaurens *et al.*, 2008). Limited transcriptional analysis in Brassica and Arabidopsis suggests that dominance in pistils is not associated with *SRK* expression differences, but again the number of interactions tested has remained limited (Suzuki et al. 1999; Kusaba et al. 2002).

Here, we take advantage of the fact that dominance interactions in Arabidopsis SI are controlled in pollen by a diversity of sRNAs and the diversity of their target sites to determine the base-pairing requirements for successful small-RNA mediated transcriptional silencing of recessive *SCR* alleles in plants with controlled S-locus genotypes. We first developed and validated a protocol for qPCR expression analysis of a set of *SCR* and *SRK* alleles in *A. halleri*. We then analysed the expression dynamics across four flower

223 developmental stages of nine *SCR* and five *SRK* alleles and tested
224 the transcriptional control of dominance for both genes in many
225 heterozygote combinations. We quantified the strength of silencing
226 of recessive *SCR* alleles and propose a quantitative threshold
227 model for how sequence identity between the small non-coding
228 RNAs and their target sites results in silencing. We discuss the
229 implications of this model on the evolutionary processes associated
230 with the origin and maintenance of the S-locus dominance
231 hierarchy in Brassicaceae.

232

233 Material & Methods

234 Plant material

235 We used a collection of 88 *A. halleri* plants containing nine
236 different S-alleles (S1, S2, S3, S4, S10, S12, S13, S20, and S29) in
237 a total of 37 of all 45 possible homozygous and heterozygous
238 combinations. Each plant was genotyped at the S-locus using the
239 PCR-based protocol described in Llaurens et al. (2008). The plants
240 were obtained by controlled crosses (Llaurens *et al.*, 2008; Durand
241 *et al.*, 2014; Leducq *et al.*, 2014) and in a few instances were
242 cloned by cuttings. Hence, a given S-locus genotype can be either
243 represented in the collection by different clones (identical genetic
244 background) or by offspring from crosses of distinct parental

origins (different genetic backgrounds). Below we refer to these two levels of experimental replicates as "clone replicates" and "biological replicates", respectively. On average, the collection comprises n= 2.05 biological replicates per S-locus genotype and clone replicates were available for three different S-locus genotypes (Table S1 & S2). The pairwise dominance interactions between these alleles as determined by pollen and pistil compatibility phenotypes of heterozygote plants are reported in Table S3.

RNA extraction and reverse transcription

On each plant, we collected flower buds at four developmental stages: 1) five highly immature inflorescence extremities (more than 2.5 days before opening, buds below 0.5mm, stages 1-10 in *A. thaliana* according to Smyth *et al.*, 1990), 2) ten immature buds (2.5 days before opening, between 0.5 and 1mm, approximately stage 11), 3) ten mature buds (one day before opening, longer than 1mm, approximately stage 12), and 4) ten open flowers (approximately stages 13-15). These stages were characterized by establishing the size distribution within each stage and measuring the time to flower opening based on ten buds. Samples collected were flash-frozen in liquid nitrogen, then stored at - 80°C before RNA extraction. Tissues were finely ground with a FastPrep-24 5G Benchtop Homogenizer (MP Biomedicals, Model #6004-500)

equipped with Coolprep 24 x 2mL adapter (6002-528) and FastPrep Lysis Beads & Matrix tube D. Total RNAs were extracted with the Arcturus "Picopure RNA isolation" kit from Life Science (PN: KIT0204) according to the manufacturer's protocol, including a step of incubation with DNAse to remove gDNA contamination. We normalized samples by using 1 mg of total RNA to perform reverse-transcription (RT) using the RevertAid Fermentas enzyme following the manufacturer's instructions.

Primer design

A major challenge to study expression of multiple S-alleles is the very high levels of nucleotide sequence divergence among them, precluding the possibility of designing qPCR primers that would amplify all alleles of the allelic series (both for *SRK* and *SCR*). Hence, we rather designed qPCR primers specifically targeted towards each of the *SCR* and *SRK* alleles, and for each heterozygote genotype we independently measured expression of both alleles of each gene. Primers were designed based on genomic sequences from BAC clones (Goubet et al 2012; Durand et al. 2014; Novikova et al. 2017), with a length of ~20 nucleotides, a GC content around 50% and a target amplicon size of 200nt. Whenever possible, we placed primers on either side of the *SCR* intron to identify and discard amplification from residual gDNA.

291 However, because the coding sequence of the *SCR* gene is short,
292 the number of possible primers was limited and this was not
293 always possible. In two cases (*SCR01* and *SCR20*), both primers
294 were thus located in the same exon. For *SRK* alleles, the primers
295 were designed on either side of the first intron. To obtain relative
296 expression levels across samples, we used *actin 8* as a
297 housekeeping gene for standardization after we verified that the *A.*
298 *thaliana* and *A. halleri* sequences are identical at the primer
299 positions (An et al. 1996). Primer sequences are reported in Table
300 S4.

301 ## Quantitative real-time PCR

302 On each cDNA sample, at least three qPCR reactions (referred to
303 below as "technical" replicates) were performed for *actin 8* and for
304 each of the S-alleles contained in the genotype (one S-allele for
305 homozygotes, two S-alleles for heterozygotes). The runs were
306 made on a LightCycler480 (Roche) with iTaq Universal SYBR
307 Green Supermix (Bio-rad, ref 172-5121). Amplified cDNA was
308 quantified by the number of cycles at which the fluorescence signal
309 was greater than a defined threshold during the logarithmic phase
310 of amplification using the LightCycler 480 software release 1.5.0
311 SP3. The relative transcript levels are shown after normalisation
312 with actin amplification through the comparative $2^{-\Delta Ct}$ method
313 (Livak & Schmittgen, 2001). The Ct_{SCR} and Ct_{SRK} values of each

314 technical replicate were normalized relative to the average Ct_{actin}
315 measure across three replicates.

316 ## Validation of qPCR primers at the dilution limits

317 Given the very large nucleotide divergence between alleles of
318 either *SCR* or *SRK*, cross-amplification is unlikely. However, to
319 formally exclude that possibility, we first performed cross-
320 amplification experiments by using each pair of *SCR* primers on a
321 set of cDNA samples that did not contain that target *SCR* allele but
322 instead contained each of the other *SCR* alleles present in our
323 experiment.

324 In order to evaluate our ability to measure expression of *SCR*
325 alleles in biological situations where they are expected to be
326 transcriptionally silenced, we then used a series of limit dilutions
327 to explore the loss of linearity of the relationship between *Ct* and
328 the dilution factor. We used six to eight replicates per dilution level
329 to evaluate the linearity of the amplification curve. Then we
330 examined the shape of the melting curves to determine whether our
331 measures at this limit dilution reflected proper PCR amplification
332 or the formation of primer dimers. Finally, we used water in place
333 of cDNA to evaluate the formation of primer dimers in complete
334 absence of the target template DNA.

Expression dynamics and the effect of dominance

We used generalized linear mixed models (lme4 package in *R*; Bates *et al.*, 2014) to decompose *Ct* values normalized by the *actin 8* control (as the dependent variable) into the effects of five explanatory variables: biological and clone replicates -reflecting the hierarchical structure of our dataset-, developmental stage, dominance phenotype and allelic identity (Table S5). Because expression of the different *SCR* (and *SRK*) alleles was quantified by different primer pairs with inevitably different amplification efficiencies, *Ct* values cannot be directly compared across alleles. Most analyses were thus performed by comparing expression levels of a given focal allele in different contexts (e.g. different genotypic contexts, different developmental stages) and accordingly we considered the identity of *SCR* or *SRK* alleles as nuisance parameters in our statistical model by including them as random effects. We visually examined normality of the residuals of the model under different distributions of $2^{-\Delta Ct}$, including Gaussian, Gamma and Gaussian with logarithmic transformations. We then tested the effect of developmental stages and dominance on *SCR* and *SRK* expression by considering them as fixed effects. Phenotypic pairwise dominance relationships were obtained from Llaurens *et al.*, (2008) and Durand *et al.*, (2014), and a set of additional controlled crosses performed following the same

protocol (Table S3). Pollen and pistil dominance relationships were used to assess the effect of dominance on *SCR* and *SRK*, respectively. To test whether the different S-alleles have distinct expression profiles across developmental stages, as suggested by Kusaba *et al.* (2002) in *A. lyrata,* we used ANOVA to compare nested models in which a random effect for the interaction between the "allelic identity" and "stage" effects was introduced.

Target features and silencing effect.

We then sought to determine how the expression of *SCR* alleles was affected by specific features of the small RNA-target interactions between alleles within heterozygote genotypes. We first used the small RNA sequencing data in Durand *et al.* (2014) and Novikova *et al.* (2017) to identify the populations of 18-26nt small RNA molecules produced by the small RNA precursors carried at the S-locus by each of the nine S-alleles. For each heterozygote combination, we then predicted the presence of putative target sites of the small RNAs produced by one S-allele on the genomic sequence of the *SCR* gene of the other S-allele including 2kb of nucleotide sequence upstream and downstream of *SCR* using a dedicated alignment algorithm and scoring matrix, as described in Durand *et al.* (2014). The reciprocal analysis was also performed regardless of the dominance relationship. Briefly, alignment quality was assessed by a scoring system based on the

addition of positive or negative values for properly paired nucleotides (+1), mismatches and gaps (-1), taking into account the non-canonical G:U interaction (-0.5). For each pair of alleles considered, only the sRNA/target combination with the highest score was selected for further analysis (Table S6). We used Akaike Information Criteria (AIC) to compare how well different base-pairing scores for target site identification predicted the level of *SCR* expression (and hence the silencing phenomenon), varying the threshold from 14 to 22. Lower values of AIC are associated with a best fit of the model. We then added a new fixed effect in our model to test whether targets in the promoter or in the intron of the *SCR* gene were associated with different strengths of silencing. For this analysis, we included only targets above the threshold identified (score >= 18).

To determine whether the base-pair requirement for silencing were identical between Brassica and Arabidopsis, we calculated the alignment score with our method between *Smi* & *Smi2* sRNAs and their targets sites in the class II alleles in *Brassica rapa* (Tarutani *et al.*, 2010, Yasuda *et al.*, 2016).

Finally, we used the phylogeny in Durand *et al.* (2014) to classify sRNA/target interactions into “ancient” (mir867 and mirS4) and “recent” (mirS1, mirS2 mirS3, mirS5, mir1887 and mir4239). Based on this classification, we used a linear regression to compare

404 the alignment score for recent and ancient sRNAs in order to test
405 the hypothesis that interactions with base-pairing scores above the
406 threshold at which silencing was apparently already complete
407 correspond to recently emerged interactions that did not yet have
408 time to accumulate mismatches.

409 # Results

410 ## Validation of the qPCR protocol and the allele-
411 ## specific primers

412 Melting curves confirmed proper amplification and low primer
413 dimers formation unless template DNA concentration was very
414 low (data not shown). The specificity test confirmed the absence of
415 cross-amplification between alleles, as the *Ct* measures for water
416 control and cross amplification were comparably high (around
417 *Ct*=34) and both were higher than the positive controls (median
418 *Ct*=22, Figure S1). For each allele tested, we then evaluated the
419 linearity of *Ct* values through serial dilutions of the template
420 cDNA. Overall, the range of variation of *Ct* values spanned by a
421 given allele across the different developmental stages or
422 dominance status was generally well within the range over which
423 *Ct* varied mostly linearly with template cDNA concentration,
424 suggesting high power to detect these effects. For *SCR*, linearity
425 was good throughout most of the dilution range, but was lost as

426 expected at very low concentration (in particular for alleles *SCR01*,
427 *SCR02*, *SCR04*, *SCR13* and *SCR20*, Figure S2a). We note that
428 comparing levels of expression for a given allele between different
429 recessive contexts (*e.g.* when silenced by different sRNAs) should
430 therefore be challenging, especially for the above-mentioned
431 alleles. Linearity was good for most *SRK* alleles (Figure S2b)
432 except for *SRK12* (data not shown), so this allele was excluded
433 from further analyses.

434 ## *SCR* and *SRK* expression dynamics across flower
435 ## development stages

436 In total, we performed 344 RNA extractions and RT-PCR from the
437 37 different S-locus genotypes sampled at four developmental
438 stages and measured 1,838 $Ct_{SCR}/Ct_{\text{actin}}$ expression ratios, resulting
439 in an average of 26.9 measures of each S-allele for each diploid
440 genotype when combining clone, biological, and technical
441 replicates and 480 $Ct_{SRK}/Ct_{\text{actin}}$ (Table S1, Table S2). Distribution
442 of the residues of the generalized mixed linear model was closest
443 to normality after log-transformation of the ratios (Figure S3). As
444 expected, measured expression levels were more highly repeatable
445 across clones than across biological replicates for a given S-locus
446 genotype, but these sources of variation were minor as compared
447 to the technical error and the allele's expression dynamic in our
448 experiment (deviance estimates of 0.40, 1.07 and 6.08 and 4.56

449 respectively, Table S5a) after taking allele identity, developmental
450 stage and dominance status into account. To determine the
451 expression dynamics of the different *SCR* alleles, we focused on
452 genotypes in which a given focal allele was known to be dominant
453 at the phenotypic level (Figure 1a). Overall, we observed a
454 consistent pattern of variation among stages (F-value: 13.805, p-
455 value: 1.107e-05, Table S5c) with a very high expression in buds
456 at early developmental stages (<0.5 to 1mm), and low level of
457 expression in late buds right before opening and in open flowers,
458 consistent with degeneration in these stages of the anther tapetum
459 where *SCR* is expected to be expressed. Accordingly to Kusaba *et*
460 *al.*, (2002), we found evidence that the expression dynamics varied
461 across alleles (Chi^2: 217.32, p-value < 2.2e-16, Table S5b). The
462 *SRK* alleles had sharply distinct dynamics of expression, with
463 monotonously increasing expression in the course of flower
464 development (Chi^2: 6.9103, p-value 0.00857, Table S5g), with
465 lowest expression in immature buds (<0.5mm) and highest
466 expression in open flowers (Figure 1b).

467 Transcriptional control

468 Based on these results, we compared expression of *SCR* alleles
469 across genotypes by averaging $2^{-\Delta Ct}$ values across <0.5mm to 1mm
470 stages. Beside a few exceptions (see below), our expression data
471 were largely consistent with the hypothesis of transcriptional

472 control of the dominance hierarchy in pollen (31 of 37 genotypic
473 combinations, Figure 2). In the four S-alleles for which
474 homozygote genotypes were available (S1, S2, S3 and S20), *SCR*
475 alleles had substantial expression in homozygotes and this was the
476 only case where expression of the most recessive allele (*SCR*01)
477 could be detected. One of the two biological replicates for the
478 S1S1 homozygote genotype had consistently low expression across
479 two clone replicates (Figure S4), so we carefully confirmed
480 homozygosity of these two samples by analysing segregation after
481 crossing to plants that did not carry S1 (all of 58 tested progenies
482 indeed carried S1 as determined by PCR on gDNA). Climbing up
483 the dominance hierarchy from most recessive to most dominant,
484 the S-alleles measured were expressed in an increasing number of
485 heterozygous combinations. At the top of the dominance hierarchy,
486 the two most dominant alleles, *SCR*13 and *SCR*20, were expressed
487 in all heterozygous contexts, including when they formed a
488 heterozygote combination with one another (S13S20), as expected
489 given the codominance observed between them at the phenotypic
490 level (Durand *et al.*, 2014). This general rule had a few exceptions
491 however (Figure 2). For instance, we detected some expression for
492 both *SCR02* and *SCR*29 in heterozygote combination even though
493 phenotypic data indicate that S2>S29 in pollen (Table S3). We also
494 observed low expression for *SCR*10 and *SCR*12 when they were in

heterozygote combination with *SCR*01 and the absence of expression for both *SCR*10 and *SCR*12 in the heterozygote combination they formed together, which is not consistent with the documented phenotypic dominance of these two alleles over *SCR*01 and between them (*SCR*12>*SCR*10; see Table S3). We confirmed proper phenotypic expression of S12 in pollen produced by the S10S12 genotype, as five replicate pollinations on a S1S12 plant produced no silique.

Overall, in spite of these six exceptions, we observed a striking contrast in transcript levels for a given allele according to its relative phenotypic dominance status in the genotype, with at least an overall 145-fold increase in transcript abundance in genotypes where a given focal allele was phenotypically dominant as compared to genotypes in which the same focal allele was recessive at stages when *SCR* is expressed (F-value: 38.582; p-value: < 2.2e-16, Table S5c). In most cases, the recessive allele came close to or even below the detection limits of our method as determined by the break of linearity of the dilution experiment (Figure S1), so this fold-change value is probably under-estimated. In strong contrast, we found no significant effect of dominance in pistils on *SRK* expression (F-value: 6.8884 p-value: 0.068244; Figure 3, Table S5h), confirming the absence of transcriptional control of dominance for *SRK*.

Target features and silencing effect

Levels of *SCR* expression of any given focal allele varied sharply with the alignment score of the "best" target available for the repertoire of sRNAs produced by the other allele present in the genotype (Figure 4a). Specifically, we observed high and variable expression of *SCR* when the score of its best predicted target was low, but consistently low *SCR* expression when the score of the best target was high (Figure 4a, Table S5d). Strikingly, the transition between high expression and low expression was very abrupt (around an alignment score of 18), suggesting a threshold effect rather than a quantitative model for transcriptional silencing. In three cases, the presence of a target with a high score within the *SCR* gene of the dominant allele was associated with high relative *SCR* expression (in agreement with the dominant phenotype), suggesting the absence of silencing in spite of the presence of a target with high sequence similarity to the sRNA produced by the recessive allele (sRNA from Ah03 on *SCR29*, score =18.5; sRNA from Ah04 on *SCR20*, score=20; and sRNA from Ah10 on *SCR20*, score =21; Figure 5a). Examining these targets in detail did not reveal mismatches at the 10-11th nucleotide position, suggesting that mismatches at other positions have rendered these sRNA-target interactions inactive (Figure 5a). Another exception concerns the observed low score (15.5) for the best match between

a sRNA from the dominant allele Ah04 and a target at *SCR* from the recessive Ah03 allele (Figure 5b). Whether Ah04 silences *SCR* from Ah03 through this unusual target or through another elusive mechanism remains to be discovered. In spite of the generally very low expression of all recessive alleles, we found some evidence that the strength of silencing experienced by a given *SCR* allele may vary across genotypic combinations for a given allele (F-value=2.222, p-value = 0.0756, Table S5i). However, we found no evidence that the position of the target site on the measured allele (promoter; intron; intron-exon boundary *vs.* upstream/downstream) could explain this variation (F-value=1.4432, n.s, TableS5e). The alignment scores obtained in Brassica for *Smi* & *Smi2* on *SCR* sequences show that dominant interactions are also strictly distinct from recessive interactions, but at a threshold score of 16.5, hence lower than that we observed in Arabidopsis (Table S6). Finally, we found no effect of the inferred age of the miRNA on the mean alignment score (mean= 20.41 and 20.22 for recent or ancient miRNAs, respectively; F-value: 0.0362; ns, Table S5j).

Discussion

Our main objective was to evaluate the base-pairing requirement of the sRNA-target interactions controlling dominance/recessivity

563 interactions between alleles of the allelic series controlling SI in *A.*
564 *halleri*. Determining the base-pairing requirement for sRNA
565 silencing in plants has remained challenging because the "rules"
566 used for target prediction have typically been deduced from
567 observations that conflate distinct microRNA genes and their
568 distinct mRNA targets over different genes. Moreover, detailed
569 evaluations of the functional consequences of mismatches have
570 relied on heterologous reporter systems (typically GFP in transient
571 tobacco assays), hence limiting the scope of the phenotypic
572 consequences that can be studied. Here, we used a genetic system
573 (plant self-incompatibility) where multiple sRNAs regulate target
574 sites on a single gene (*SCR*), and in which we are able to make a
575 direct link between the sRNA-target interactions, the level of *SCR*
576 transcript and the encoded phenotype (dominance/recessivity
577 interaction).

578 The first step was to clarify several aspects of the expression
579 pattern of the genes controlling SI in *A. halleri,* as earlier accounts
580 had suggested that alleles of the allelic series may differ from one
581 another in their expression profile (Kusaba *et al.*, 2002). In line
582 with Kakizaki *et al.*, (2003), Suzuki *et al.*, (1999); Schopfer *et al.*,
583 (1999); Takayama *et al.*, (2000); Shiba *et al.*, (2002),we found
584 maximal expression of *SCR* in early buds but low or no expression
585 at the open flower stage. This expression pattern is consistent with

586 *in situ* hybridization experiments showing that *SCR* transcripts are
587 localized in the tapetum, a specialized layer of cells involved in
588 pollen grains coating (Iwano *et al.*, 2003), which undergoes
589 apoptosis and is quickly degraded as the development of pollen
590 grains inside the anther progresses (Murphy & Ross, 1998;
591 Takayama *et al.*, 2000). We confirmed that differences exist in the
592 temporal dynamics of expression among alleles, as suggested by
593 Kusaba *et al.* (2002) in *A. lyrata*, possibly as the result of strong
594 sequence divergence of the promotor sequences of the different
595 *SCR* alleles. Finally, we confirmed that *SCR* and *SRK* have sharply
596 distinct expression dynamics throughout flower development.
597 Indeed, transcript levels of *SRK* increased steadily along
598 development and were very low in early buds, consistent with the
599 observation that SI can be experimentally overcome to obtain
600 selfed progenies by “bud-pollination” (Llaurens et al. 2009).

601 Based on this clarified transcriptional dynamics, we confirmed the
602 generality of the transcriptional control of dominance for *SCR*. In
603 particular, we observed that even in the few heterozygote
604 genotypes where in our previous study (Durand *et al.*, 2014) no
605 sRNA produced by the phenotypically dominant allele was
606 predicted to target the sequence of the phenotypically recessive
607 *SCR* allele, transcripts from the recessive *SCR* allele were
608 undetected. This suggests either that some functional sRNAs or

609 targets have remained undetected by previous sequencing and/or
610 by our *in silico* prediction procedures, or that mechanisms other
611 than sRNAs may cause transcriptional silencing for some S-allele
612 combinations. In contrast, we confirmed the absence of
613 transcriptional control for *SRK*, for which both alleles were
614 consistently expressed at similar levels in all heterozygote
615 genotypes examined, irrespective of the (pistil) dominance
616 phenotype. For *SRK*, other dominance mechanisms must therefore
617 be acting, which are yet to be discovered (*e.g.* Naithani *et al.*,
618 2007).

619 An important feature of the silencing phenomenon is that the
620 decrease of transcript levels for recessive *SCR* alleles was very
621 strong in heterozygous genotypes, bringing down transcript levels
622 below the limits of detection in most cases. This is in line with the
623 intensity of transcriptional silencing by heterochromatic siRNAs
624 (typically very strong for transposable element sequences, see
625 Marí-Ordóñez *et al.*, 2013), while post-transcriptional gene
626 silencing by microRNAs is typically more quantitative (Liu *et al.*,
627 2014). As a result of this strong decrease of transcript levels, the
628 strength of silencing appeared independent from the position of the
629 sRNA target along the *SCR* gene (promoter *vs.* intron), although
630 we note that our power to distinguish among levels of transcripts
631 of recessive alleles, which were all extremely low, is itself fairly

low. It remains to be discovered whether the different positions of the sRNA targets do indeed imply different transcriptional silencing mechanisms (Durand *et al*., 2014).

Based on the many allelic combinations where we could compare the agnostic prediction of putative target sites with the level of transcriptional silencing, we find that a simple threshold model for base-pairing between sRNAs and their target sites captures most of the variation in *SCR* expression in heterozygotes. This result provides a direct experimental validation of the *ad-hoc* criteria used in Durand *et al.*, (2014). However, our results also indicate that this quantitative threshold is not entirely sufficient to capture the complexity of targeting interactions. Indeed, in two cases for which the dominance relationship is known, this simple threshold model would inappropriately predict that sRNAs from recessive alleles should be able to target more dominant *SCR* alleles, yet the dominant *SCR* alleles were expressed at normal levels with no sign of silencing in these heterozygote genotypes (Figure 5a). The position of the mismatches on these sRNAs (at position 15 and 18 of the sRNA for Ah03 on Ah29, and position 3 and 12 for the others) therefore appear to be sufficient to abolish the function of the targeting interaction. Similarly, a mismatch at position 10 in the *Smi* interaction in Brassica (Tarutani *et al.*, 2010) and in other microRNA-targets interactions (Franco-Zorrilla *et al.*, 2007) was

655 shown to result in loss of function of the interaction (Table S6).
656 Interestingly, quantitative differences may exist between
657 Arabidopsis and Brassica, as the experimentally validated targets
658 in Brassica (Tarutani *et al.*, 2010; Yasuda *et al.*, 2016) correspond
659 to base-pairing threshold below the one that we find in Arabidopsis
660 (*i.e.* a target score of 16.5 seems sufficient for silencing in Brassica
661 *vs.* 18 in Arabidopsis). For Brassica, both class I and class II alleles
662 have *Smi*, but a mismatch at the 10th position was proposed to
663 explain why the class II *Smi* is not functional. Here, we found that
664 this mismatch drives the alignment score under the 16.5 threshold
665 and could be sufficient to explain the loss of function, regardless of
666 its position. Overall, although these small RNAs achieve their
667 function in a way that is sharply different from classical
668 microRNAs (DNA methylation *vs.* mRNA cleavage), our results
669 suggest that the sRNA-target complementarity rules for silencing
670 in both cases are qualitatively consistent (Liu *et al.*, 2014). Better
671 understanding the molecular pathway by which these sRNAs
672 epigenetically silence their target gene (*SCR*) will now be key to
673 determine whether this threshold model can be generalized to more
674 classical siRNAs found across the genome, as evidence is still
675 missing for such classes of sRNAs.

676 The existence of a threshold model has important implications for
677 how the dominance hierarchy can evolve. In fact, our model

678 suggests that a single SNP can be sufficient to turn a codominance
679 interaction into a dominance interaction (and vice-versa), making
680 this a relatively trivial molecular event. This is actually what
681 Yasuda *et al.*, (2016) observed in *B. rapa*, where the combination
682 of single SNPs at the sRNA *Smi2* and its *SCR* target sequences
683 resulted in a linear dominance hierarchy among the four class II S-
684 alleles found in that species. Strikingly, in some cases, we
685 observed base pairing at sRNA-target interactions with very high
686 alignment scores (up to 22), *i.e.* above the threshold at which
687 transcriptional silencing was already complete (score =18). Under
688 our threshold model, such interactions are not expected since
689 complete silencing is already achieved at the threshold, and no
690 further fitness gain is therefore to be expected by acquiring a more
691 perfect target. A first possibility is that these interactions reflect the
692 recent emergence of these silencing interactions. In fact, one of the
693 models for the emergence of new microRNAs in plant genomes
694 involves a partial duplication of the target gene, hence entailing
695 perfect complementarity at the time of origin that becomes
696 degraded over time by the accumulation of mutations (Allen *et al.*,
697 2004). Under this scenario, the higher-than-expected levels of
698 sRNA-target complementarity could reflect the recent origin of
699 these sRNAs but we found no evidence of a difference in
700 alignment score for young *vs.* old microRNAs (Table S5j). A

second possibility is that selection for developmental robustness is acting to prevent the phenotypic switch from mono- to bi-allelic expression of *SCR* (especially during stress events, Boukhibar & Barkoulas, 2016) that could be devastating for the plant reproductive fitness. Indeed, we do observe strong variation in overall *SCR* expression when the sRNA target score of the companion allele is below the threshold, and it is possible that under stress conditions the epigenetic machinery may be less efficient, hence requiring stronger base-pairing to achieve proper silencing than in the greenhouse conditions under which we observed them in the present study. Finally, a third possibility is that sRNA-target complementarity above the threshold reflects the pleiotropic constraint of having a given sRNA from a dominant allele control silencing of the complete set of target sequences from the multiple recessive alleles segregating, and reciprocally of having a given *SCR* target in a recessive allele maintaining molecular match with a given sRNA distributed among a variety of dominant alleles. Comparing the complementarity score of sRNA/target interactions among sRNAs or targets that contribute to high versus low numbers of dominance/recessive interactions will now require a more complete depiction of the sRNA-target regulatory network among the larger set of S-alleles segregating in natural populations.

724

725 Acknowledgments

726 We thank Sylvain Billiard and Isabelle de Cauwer for statistical
727 advice and discussions, Romuald Rouger and Anne Duputié for
728 help with producing figures and Alexis Sarazin for comments on
729 the manuscript. This work was funded by the European Research
730 Council (NOVEL project, grant #648321). N.B. was supported by
731 a doctoral grant from the president of Université de Lille-Sciences
732 et Technologies and the French ministry of research. The authors
733 also thank the Région Hauts-de-France, and the Ministère de
734 l'Enseignement Supérieur et de la Recherche (CPER Climibio),
735 and the European Fund for Regional Economic Development for
736 their financial support.

737

738 Author Contribution

739 NB, SS, SB, ACH performed the molecular biology experiments.
740 CP and ES obtained and took care of the plants. SS, IFL and XV
741 provided advice on the experimental strategy and interpretations.
742 NB performed the statistical analyses. VC supervised the work.
743 NB and VC wrote the manuscript.

744

References cited

Aalto AP, Pasquinelli AE. **2012**. Small non-coding RNAs mount a silent revolution in gene expression. *Current Opinion in Cell Biology* **24**: 333–340.

Allen E, Xie Z, Gustafson AM, Sung GH, Spatafora JW, Carrington JC. **2004**. Evolution of microRNA genes by inverted duplication of target gene sequences in *Arabidopsis thaliana*. *Nature Genetics* **36**: 1282–1290.

An YQ, McDowell JM, Huang S, McKinney EC, Chambliss S, Meagher RB. **1996**. Strong, constitutive expression of the Arabidopsis ACT2/ACT8 actin subclass in vegetative tissues. *The Plant journal : for cell and molecular biology* **10**: 107–121.

Axtell MJ, Meyers BC. **2018**. Revisiting criteria for plant miRNA annotation in the era of big data. *The Plant Cell*: tpc.00851.2017.

Bates D, Mächler M, Bolker B, Walker S. **2014**. Fitting Linear Mixed-Effects Models using lme4. *Journal of Statistical Software* **67**: 1–48.

Boukhibar LM, Barkoulas M. **2016**. The developmental genetics of biological robustness. *Annals of Botany* **117**: 699–707.

Castric V, Bechsgaard J, Schierup MH, Vekemans X. **2008**. Repeated adaptive introgression at a gene under multiallelic

766 balancing selection. *PLoS Genetics* **4**.

767 **Castric V, Vekemans X**. **2004**. Plant self-incompatibility in
768 natural populations: A critical assessment of recent theoretical and
769 empirical advances. *Molecular Ecology* **13**: 2873–2889.

770 **Cuerda-Gil D, Slotkin RK**. **2016**. Non-canonical RNA-directed
771 DNA methylation. *Nature Plants* **2**: 16163.

772 **Ding J, Zhou S, Guan J**. **2012**. Finding MicroRNA Targets in
773 Plants: Current Status and Perspectives. *Genomics, Proteomics and*
774 *Bioinformatics* **10**: 264–275.

775 **Durand E, Méheust R, Soucaze M, Goubet PM, Gallina S,**
776 **Poux C, Fobis-loisy I, Guillon E, Gaude T, Sarazin A, *et al.***
777 **2014**. Dominance hierarchy arising from the evolution of a
778 complex small RNA regulatory network. *Science* **346**: 1200–1205.

779 **Fei Q, Xia R, Meyers BC**. **2013**. Phased, secondary, small
780 interfering RNAs in posttranscriptional regulatory networks. *The*
781 *Plant Cell* **25**: 2400–2415.

782 **Finnegan EJ, Liang D, Wang M**. **2011**. Self-incompatibility : *Smi*
783 silences through a novel sRNA pathway. *Trends in Plant Science*
784 **16**: 238–241.

785 **Franco-Zorrilla JM, Valli A, Todesco M, Mateos I, Puga MI,**
786 **Rubio-Somoza I, Leyva A, Weigel D, García JA, Paz-Ares J**.

2007. Target mimicry provides a new mechanism for regulation of microRNA activity. *Nature Genetics* **39**: 1033–1037.

Goubet PM, Bergès H, Bellec A, Prat E, Helmstetter N, Mangenot S, Gallina S, Holl A-C, Fobis-Loisy I, Vekemans X, *et al.* 2012. Contrasted pattern of molecular evolution in dominant and recessive self-incompatibility haplotypes in Arabidopsis. *PLoS genetics* **8**.

Hatakeyama K, Takasaki T, Suzuki G, Nishio T, Watanabe M, Isogai A, Hinata K. **2001**. The S Receptor Kinase gene determines dominance relationships in stigma expression of self-incompatibility in Brassica. *Plant Journal* **26**: 69–76.

Iwano M, Shiba H, Funato M, Shimosato H, Takayama S, Isogai A. **2003**. Immunohistochemical studies on translocation of pollen S-haplotype determinant in self-incompatibility of *Brassica rapa*. *Plant and Cell Physiology* **44**: 428–436.

Jones-Rhoades MW, Bartel DP, Bartel B. **2006**. MicroRNAs and their regulatory roles in plants. *Annual Review of Plant Biology* **57**: 19–53.

Kakizaki T, Takada Y, Ito A, Suzuki G, Shiba H, Takayama S, Isogai A, Watanabe M. **2003**. Linear dominance relationship among four class-II S haplotypes in pollen is determined by the expression of SP11 in Brassica self-incompatibility. *Plant & cell*

physiology **44**: 70–75.

Kusaba M, Dwyer K, Hendershot J, Vrebalov J, Nasrallah JB, Nasrallah ME. **2001**. Self-incompatibility in the genus Arabidopsis: characterization of the S locus in the outcrossing A. lyrata and its autogamous relative A. thaliana. *The Plant cell* **13**: 627–643.

Kusaba M, Tung C-W, Nasrallah ME, Nasrallah JB. **2002**. Monoallelic expression and dominance interactions in anthers of self-incompatible *Arabidopsis lyrata*. *Plant physiology* **128**: 17–20.

Leducq J-B, Gosset CC, Gries R, Calin K, Schmitt É, Castric V, Vekemans X. **2014**. Self-incompatibility in Brassicaceae: identification and characterization of *SRK* -like sequences linked to the S-Locus in the tribe Biscutelleae. *Genes|Genomes|Genetics* **4**: 983–992.

Li J, Reichel M, Li Y, Millar AA. **2014**. The functional scope of plant microRNA-mediated silencing. *Trends in Plant Science* **19**: 750–756.

Liu Q, Wang F, Axtell MJ. **2014**. Analysis of complementarity requirements for plant MicroRNA targeting using a Nicotiana benthamiana quantitative transient assay. *The Plant Cell* **26**: 741–753.

Livak KJ, Schmittgen TD. **2001**. Analysis of relative gene

831 expression data using real-time quantitative PCR and. *Methods* **25**:
832 402–408.

833 **Llaurens V, Billiard S, Leducq JB, Castric V, Klein EK,**
834 **Vekemans X**. **2008**. Does frequency-dependent selection with
835 complex dominance interactions accurately predict allelic
836 frequencies at the self-incompatibility locus in *Arabidopsis*
837 *halleri*? *Evolution* **62**: 2545–2557.

838 **Ma R, Han Z, Hu Z, Lin G, Gong X, Zhang H, Nasrallah JB,**
839 **Chai J**. **2016**. Structural basis for specific self-incompatibility
840 response in Brassica. *Nature Publishing Group* **26**: 1320–1329.

841 **Mable BK, Schierup MH, Charlesworth D**. **2003**. Estimating the
842 number, frequency, and dominance of S-alleles in a natural
843 population of *Arabidopsis lyrata* (Brassicaceae) with sporophytic
844 control of self-incompatibility. *Heredity* **90**: 422–31.

845 **Mallory AC, Reinhart BJ, Jones-Rhoades MW, Tang G,**
846 **Zamore PD, Barton MK, Bartel DP**. **2004**. MicroRNA control of
847 PHABULOSA in leaf development: importance of pairing to the
848 microRNA 5′ region. *The EMBO Journal* **23**: 3356–3364.

849 **Marí-Ordóñez A, Marchais A, Etcheverry M, Martin A, Colot**
850 **V, Voinnet O**. **2013**. Reconstructing *de novo* silencing of an active
851 plant retrotransposon. *Nature genetics* **45**: 1029–1039.

852 **Matzke M, Kanno T, Daxinger L, Huettel B, Matzke AJ**. **2009**.

853 RNA-mediated chromatin-based silencing in plants. *Current*
854 *Opinion in Cell Biology* **21**: 367–376.

855 **Murphy DJ, Ross JH**. **1998**. Biosynthesis, targeting and
856 processing of oleosin-like proteins, which are major pollen coat
857 components in *Brassica napus*. *Plant J* **13**: 1–16.

858 **Naithani S, Chookajorn T, Ripoll DR, Nasrallah JB**. **2007**.
859 Structural modules for receptor dimerization in the S-locus
860 receptor kinase extracellular domain. *Proceedings of the National*
861 *Academy of Sciences* **104**: 12211–6.

862 **De Nettancourt D**. **2001**. *Incompatibility and Incongruity in Wild*
863 *and Cultivated Plants*. (BY Springer-Verlag., Ed.).

864 **Novikova PY, Hohmann N, Nizhynska V, Tsuchimatsu T, Ali**
865 **J, Muir G, Guggisberg A, Paape T, Schmid K, Fedorenko OM,**
866 ***et al.*** **2016**. Sequencing of the genus Arabidopsis identifies a
867 complex history of nonbifurcating speciation and abundant trans-
868 specific polymorphism. *Nature Genetics* **48**: 1077–1082.

869 **Palazzo AF, Lee ES**. **2015**. Non-coding RNA: What is functional
870 and what is junk? *Frontiers in Genetics* **5**: 1–11.

871 **Parizotto EA, Parizotto EA, Dunoyer P, Dunoyer P, Rahm N,**
872 **Rahm N, Himber C, Himber C, Voinnet O, Voinnet O**. **2004**. In
873 vivo investigation of the transcription, processing, endonucleolytic
874 activity, and functional relevance of the spatial distribution of a

875 plant miRNA. *Genes & Development* **18(18)**: 2237–2242.

876 **Remans T, Smeets K, Opdenakker K, Mathijsen D,**
877 **Vangronsveld J, Cuypers A**. **2008**. Normalisation of real-time
878 RT-PCR gene expression measurements in Arabidopsis thaliana
879 exposed to increased metal concentrations. *Planta* **227**: 1343–
880 1349.

881 **Schopfer CR, Nasrallah ME, Nasrallah JB**. **1999**. The male
882 determinant of self-incompatibility in Brassica. *Science* **286**: 1697
883 LP-1700.

884 **Schwab R, Palatnik JF, Riester M, Schommer C, Schmid M,**
885 **Weigel D**. **2005**. Specific effects of microRNAs on the plant
886 transcriptome. *Developmental Cell* **8**: 517–527.

887 **Shiba H, Iwano M, Entani T, Ishimoto K, Shimosato H, Che F-**
888 **S, Satta Y, Ito A, Takada Y, Watanabe M, *et al.* 2002**. The
889 dominance of alleles controlling self-incompatibility in Brassica
890 pollen is regulated at the RNA level. *The Plant cell* **14**: 491–504.

891 **Shiba H, Kakizaki T, Iwano M, Tarutani Y, Watanabe M,**
892 **Isogai A, Takayama S**. **2006**. Dominance relationships between
893 self-incompatibility alleles controlled by DNA methylation. *Nature*
894 *Genetics* **38**: 297–9.

895 **Smyth DR, Bowman JL, Meyerowitz EM**. **1990**. Early flower
896 development in Arabidopsis. *The Plant Cell* **2**: 755–767.

Suzuki G, Kai N, Hirose T, Fukui K, Nishio T, Takayama S, Isogai A, Watanabe M, Hinata K. **1999**. Genomic organization of the S locus : identification and characterization of genes in SLG / SRK region of S9 haplotype of Brassica campestris (syn . rapa). *Genetics* **153(1)**: 391–400.

Takayama S, Shiba H, Iwano M, Shimosato H, Che FS, Kai N, Watanabe M, Suzuki G, Hinata K, Isogai A. **2000**. The pollen determinant of self-incompatibility in *Brassica campestris*. *Proceedings of the National Academy of Sciences of the United States of America* **97**: 1920–1925.

Tarutani Y, Shiba H, Iwano M, Kakizaki T, Suzuki G, Watanabe M, Isogai A, Takayama S. **2010**. Trans-acting small RNA determines dominance relationships in Brassica self-incompatibility. *Nature* **466**: 983–986.

Vaucheret H, Béclin C, Elmayan T, Feuerbach F, Godon C, Morel JB, Mourrain P, Palauqui JC, Vernhettes S. **1998**. Transgene-induced gene silencing in plants. *The Plant journal* **16**: 651–659.

Vazquez F, Legrand S, Windels D. **2010**. The biosynthetic pathways and biological scopes of plant small RNAs. *Trends in Plant Science* **15**: 337–345.

Wang F, Polydore S, Axtell MJ. **2015**. More than meets the eye?

Factors that affect target selection by plant miRNAs and heterochromatic siRNAs. *Current Opinion in Plant Biology* **27**: 118–124.

Wickham H. **2009**. *ggplot2: Elegant Graphics for Data Analysis.* New-York: Springer-Verlag.

Yasuda S, Wada Y, Kakizaki T, Tarutani Y, Miura-uno E, Murase K, Fujii S, Hioki T, Shimoda T, Takada Y, *et al.* 2016. A complex dominance hierarchy is controlled by polymorphism of small RNAs and their targets. *Nature Plants* **16206**: 1–6.

Figure legends

Figure 1: Expression dynamics of **a.** *SCR* and **b.** *SRK* during flower development, from early buds (<0.5mm) to open flowers. For *SCR*, only genotypes in which a given allele was either dominant or co-dominant were included (recessive *SCR* alleles were strongly silenced at all stages and were therefore not informative here). For each allele, $2^{-\Delta Ct}$ values were normalized relative to the developmental stage with the highest expression. For each stage, the thick horizontal line represents the median, the box represents the 1st and 3rd quartiles. The upper whisker extends from the hinge to the largest value no further than 1.5 * Inter Quartile Range from the hinge (or distance between the first and third

941 quartiles). The lower whisker extends from the hinge to the
942 smallest value at most 1.5 * IQR of the hinge and the black dots
943 represents outlier values.

944 **Figure 2**: Expression of individual *SCR* alleles in different
945 genotypic contexts. Pollen dominance status of the S-allele whose
946 expression is measured relative to the other allele in the genotype
947 as determined by controlled crosses are represented by different
948 letters (**D**: dominant; **C**: codominant; **R**: recessive; **U**: unknown;
949 **H**: Homozygote, Table S3). In a few instances, relative dominance
950 status of the two alleles had not been resolved phenotypically and
951 were inferred from the phylogeny (marked by asterisks). Thick
952 horizontal bars represent the median of $2^{-\Delta Ct}$ values, 1st and 3rd
953 quartile are indicated by the upper and lower limits of the boxes.
954 The upper whisker extends from the hinge to the largest value no
955 further than 1.5 * Inter Quartile Range from the hinge (or distance
956 between the first and third quartiles). The lower whisker extends
957 from the hinge to the smallest value at most 1.5 * IQR of the hinge
958 and the black dots represents outlier values. We normalized values
959 relative to the highest median across heterozygous combinations
960 within each panel. Alleles are ordered from left to right and from
961 top to bottom according to their position along the dominance
962 hierarchy, with SCR01 the most recessive and SCR13 and SCR20
963 the most dominant alleles. Under a model of transcriptional control

964 of dominance, high expression is expected when a given allele is
965 either dominant or co-dominant and low expression when it is
966 recessive. Exceptions to this model are marked by black vertical
967 arrows and discussed in the text. “Na” marks homozygote or
968 heterozygote genotypes that were not available.

969 **Figure 3:** Expression of individual *SRK* alleles in different
970 genotypic contexts. Putative pistil dominance status of the S-allele
971 whose expression is measured relative to the other allele in the
972 genotype is represented by different letters (**D**: dominant; **R**:
973 recessive; **U**: unknown; **H**: Homozygote). Note that the pistil
974 dominance hierarchy of the S-allele have been less precisely
975 determined than the pollen hierarchy, and so many of the pairwise
976 dominance interactions were indirectly inferred from the
977 phylogenetic relationships (and marked by an asterisk) rather than
978 directly measured phenotypically. Thick horizontal bars represent
979 the median of $2^{-\Delta Ct}$ values, 1st and 3rd quartile are indicated by the
980 upper and lower limits of the boxes. The upper whisker extends
981 from the hinge to the largest value no further than 1.5 * Inter
982 Quartile Range from the hinge (or distance between the first and
983 third quartiles). The lower whisker extends from the hinge to the
984 smallest value at most 1.5 * IQR of the hinge and the black dots
985 represents outlier values.. We normalized the values for each allele
986 relative to the higher median across heterozygous combination. We

normalized values relative to the highest median across heterozygous combinations within each panel. Alleles are ordered from left to right and from top to bottom according to their position in the pistil dominance hierarchy, with SRK01 the most recessive and SRK04 the most dominant allele in our sample, based on the phenotypic determination in Llaurens *et al.* (2008).

Figure 4: Base-pairing requirements for the transcriptional control of *SCR* alleles by sRNAs suggest a threshold model. **a.** Relative expression of *SCR* alleles as a function of the alignment score of the "best" interaction between the focal allele (including 2kb of sequence upstream and downstream of *SCR*) and the population of sRNAs produced by sRNA precursors of the other allele in the genotype. For each allele, expression was normalized relative to the genotype in which the $2^{-\Delta Ct}$ value was highest. Dots are coloured according to the dominance status of the focal *SCR* allele in each genotypic context (black: dominant; white: recessive; grey: undetermined). The black line corresponds to a local regression obtained by a smooth function (loess function, span=0.5) in the ggplot2 package (Wickham, 2009) and the grey area covers the 95% confidence interval. Vertical arrows point to observations that do not fit the threshold model of transcriptional control and are represented individually on Figure 5. **b.** Barplots of the Akaike Information Criteria (AIC) quantifying the fit of the generalized

linear model for different target alignment scores used to define functional targets. Lower AIC values indicate a better fit.

Figure 5: Predicted sRNA/target interactions that do not fit with the documented dominance phenotype or the measured expression. For each alignment, the sequence on top is the sRNA and the bottom sequence is the best predicted target site on the *SCR* gene sequence (including 2kb of sequence upstream and downstream of *SCR*). **a.** sRNA targets with a score above 18, while the S-allele producing the sRNA is phenotypically recessive over the S-allele containing the *SCR* sequence. **b.** sRNA target with a score below 18, while the S-allele producing the sRNA (Ah04) is phenotypically dominant over the S-allele containing the *SCR* sequence and transcript levels of the *SCR03* allele is accordingly very low. This is the best target we could identify on SCR03 for sRNAs produced by Ah04.

Supplementary figures

Figure S1. Validation of the *SCR* qPCR primers. "Positive control**"** corresponds to amplification with the Master Mix containing primers for *SCR* alleles that are present in the cDNA used. For the "Cross Amplification" assay, we used a Master Mix on cDNAs that do not contain alleles corresponding to the primer

pair used. "Water": master mix with water instead of cDNA. Thick horizontal bars represent the median of $2^{-\Delta Ct}$ values, 1st and 3rd quartile are indicated by the upper and lower limits of the. The upper whisker extends from the hinge to the largest value no further than 1.5 * Inter Quartile Range from the hinge (or distance between the first and third quartiles). The lower whisker extends from the hinge to the smallest value at most 1.5 * IQR of the hinge and the black dots represents outlier values.

Figure S2: qPCR amplification (non-transformed *Ct* values) in serial dilutions for each *SCR* (**a**) and *SRK* (**b**) allele. Solid lines are the linear regressions over all *Ct* values. Dashed lines are linear regressions excluding the highest dilution level.

Figure S3. Generalized linear mixed model used to test the effect of developmental stage and dominance status on the expression of *SCR* alleles (*Ct* values). The distribution shows that the residues of the full model are approximately normally distributed when taking allele identity, developmental stage and dominance status into account and using a logarithmic transformation of the Ct_{SCR} /Ct_{actin} ratios.

Figure S4. Expression of individual *SCR* alleles in different genotypic contexts, representing each biological and clone replicate separately. Symbols on top of the boxes indicate

measures from identical clone replicates. See legend of Figure 2 for a full description.

Table S1. *SCR* samples analysed for each S-locus genotype, showing the number of biological and clone replicates over the four developmental stages sampled. "Allele 1" refers to the first allele noted in the genotype (for example in the S1S2 genotype, "allele 1" is S1 and "allele 2" is S2).

Table S2: *SRK* samples analysed for each S-locus genotype, showing the number of biological and clone replicates over the four developmental stages sampled. The alleles are named accordingly to the Table S1.

Table S3: Dominance relationships between alleles from the different genotypes included in this study as determined by controlled crosses.

Table S4: qPCR primer sequences for each *SCR* and *SRK* alleles studied.

Table S5: Detailed results from the generalized linear mixed models. **a**. Decomposition of the sources of variance across allele identity and the hierarchical levels biological, clones and technical replicates for *SCR*. **b**. Test of the variation of expression dynamic across *SCR* alleles. **c**. Test of the dominance and stage effects on *SCR* transcript levels, showing a significant interaction. **d**.

1076 Comparison of the fit of the model under different base-pairing
1077 score thresholds. **e**. Test of the effect of the position of the target
1078 on the strength of silencing. **f**. Decomposition of the source of
1079 variance across the technical replicates and the allele identity for
1080 *SRK*. **g**. Test of the variation of expression dynamic across *SRK*
1081 alleles. **h.** Test of the effect of stage and dominance on *SRK*
1082 transcript levels. **i**. Test of the effect of the identity of the
1083 companion allele on *SCR* transcript levels. **j**: Test of the effect of
1084 age on alignment score above the threshold of 18.

1085 **Table S6:** sRNA and target identified as the best match for every
1086 pair of alleles for *SCR*. Ct_{SCR}/Ct_{actin} ratios are given for the target
1087 allele in the interaction, calculated from the mean of Ct_{SCR}/Ct_{actin}
1088 ratios across the two earliest developmental stages (buds below
1089 1mm, see Figure 1). The positions of the targets are given relative
1090 to the beginning of the closest exon of *SCR* for targets upstream
1091 from the gene or in the intron), and relative to the stop codon for
1092 downstream targets. R: Recessive; D: dominant; H: homozygote.

Figure 1

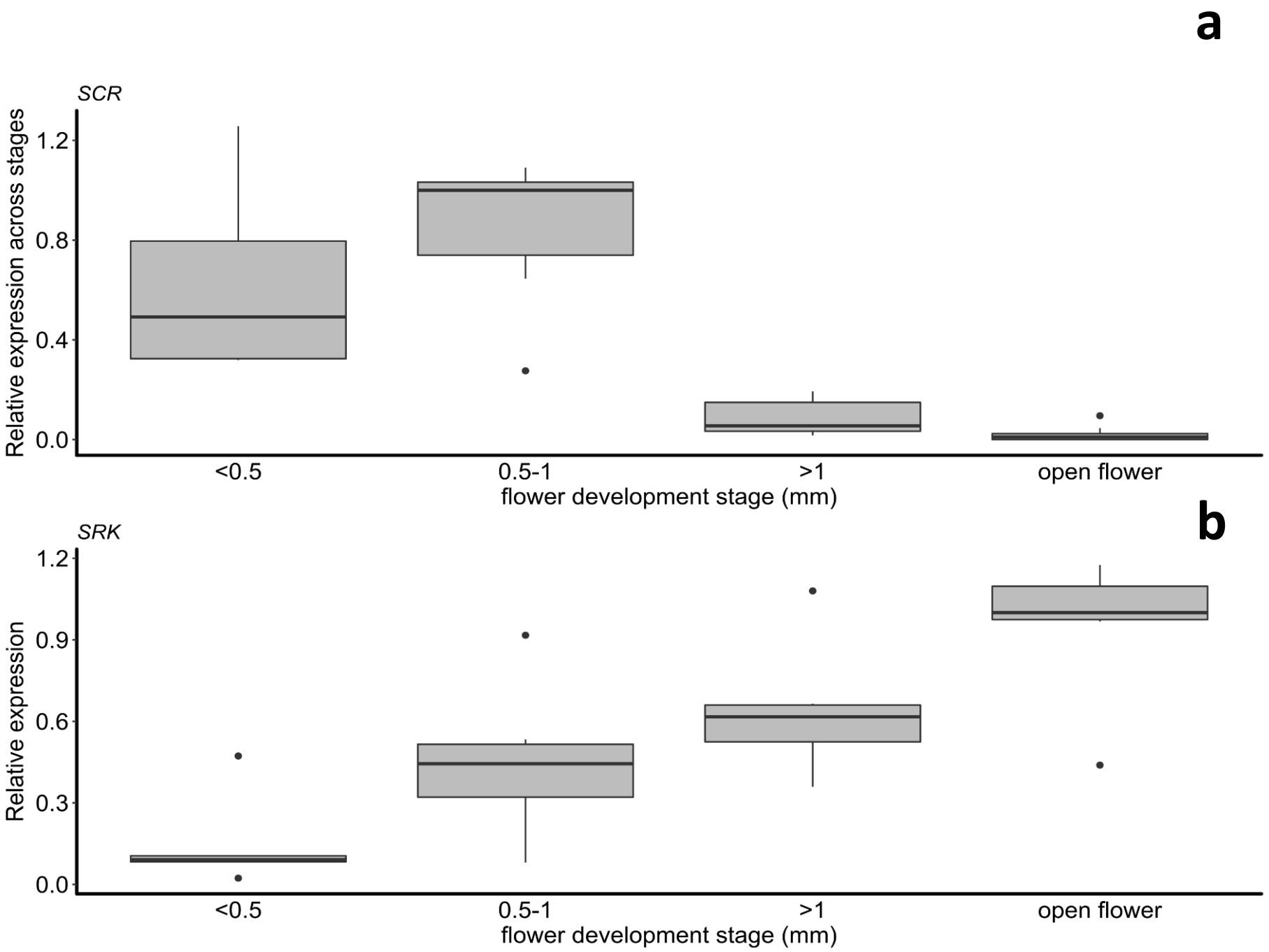

Figure 2

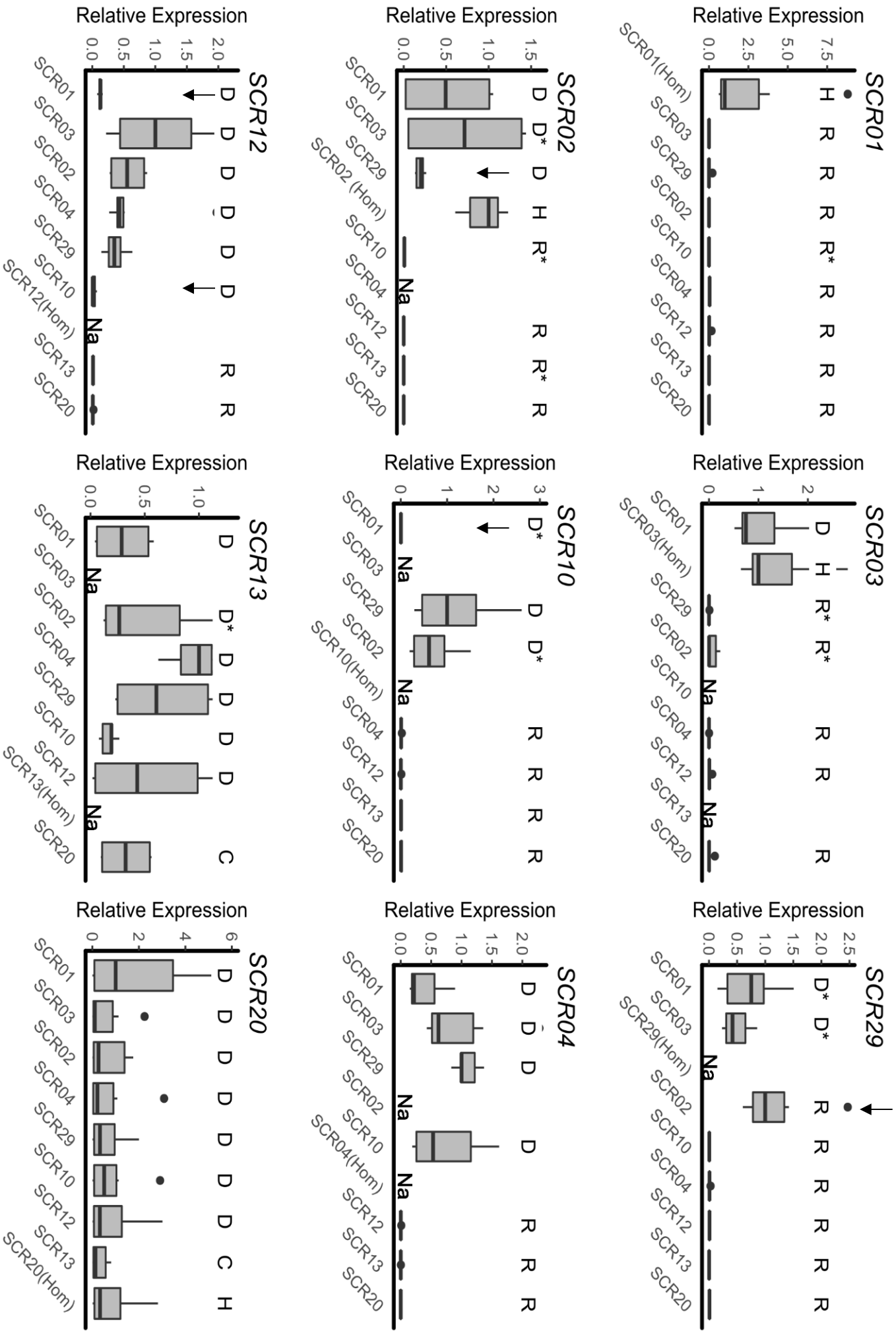

Figure 3

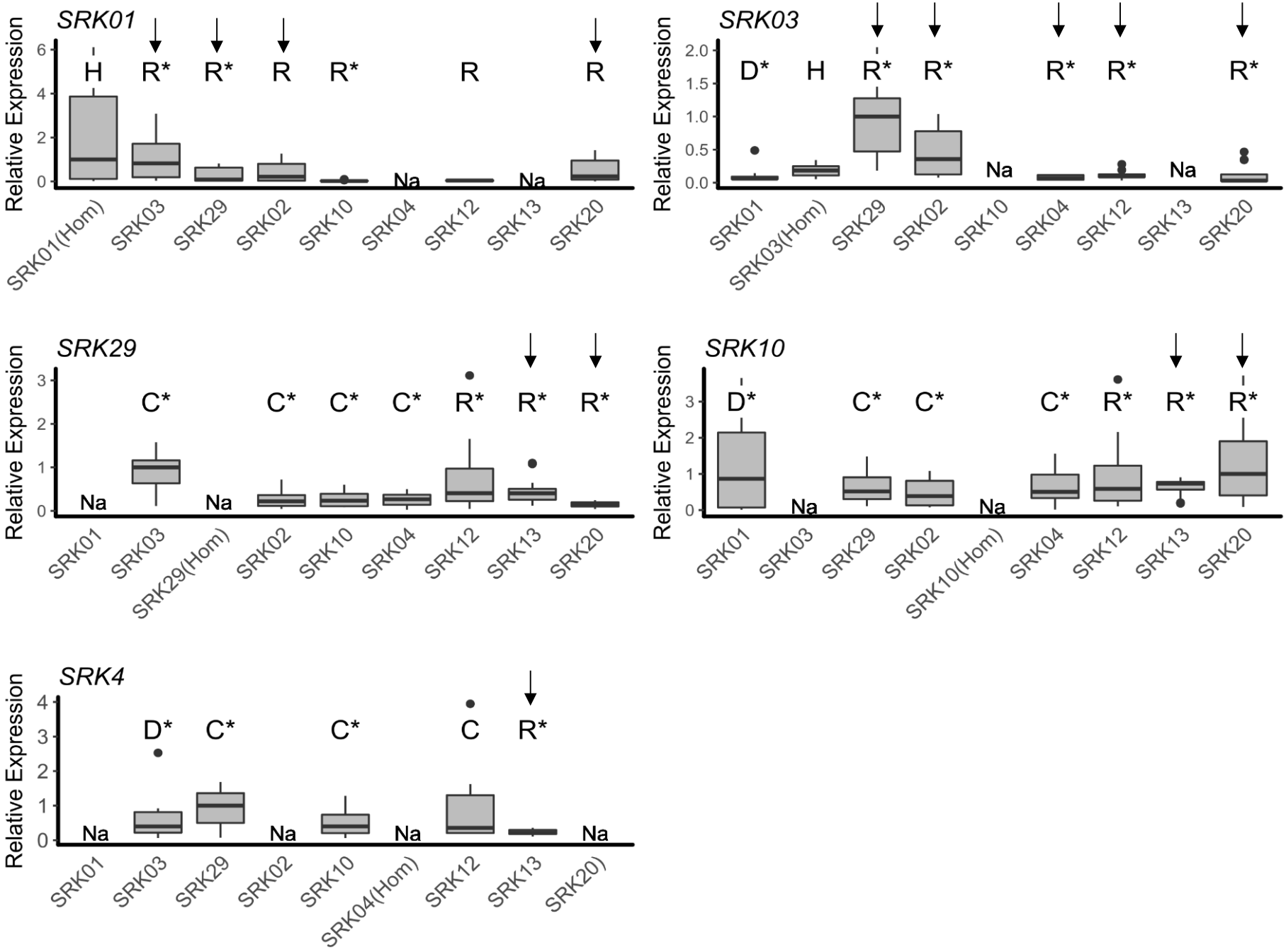

Figure 4

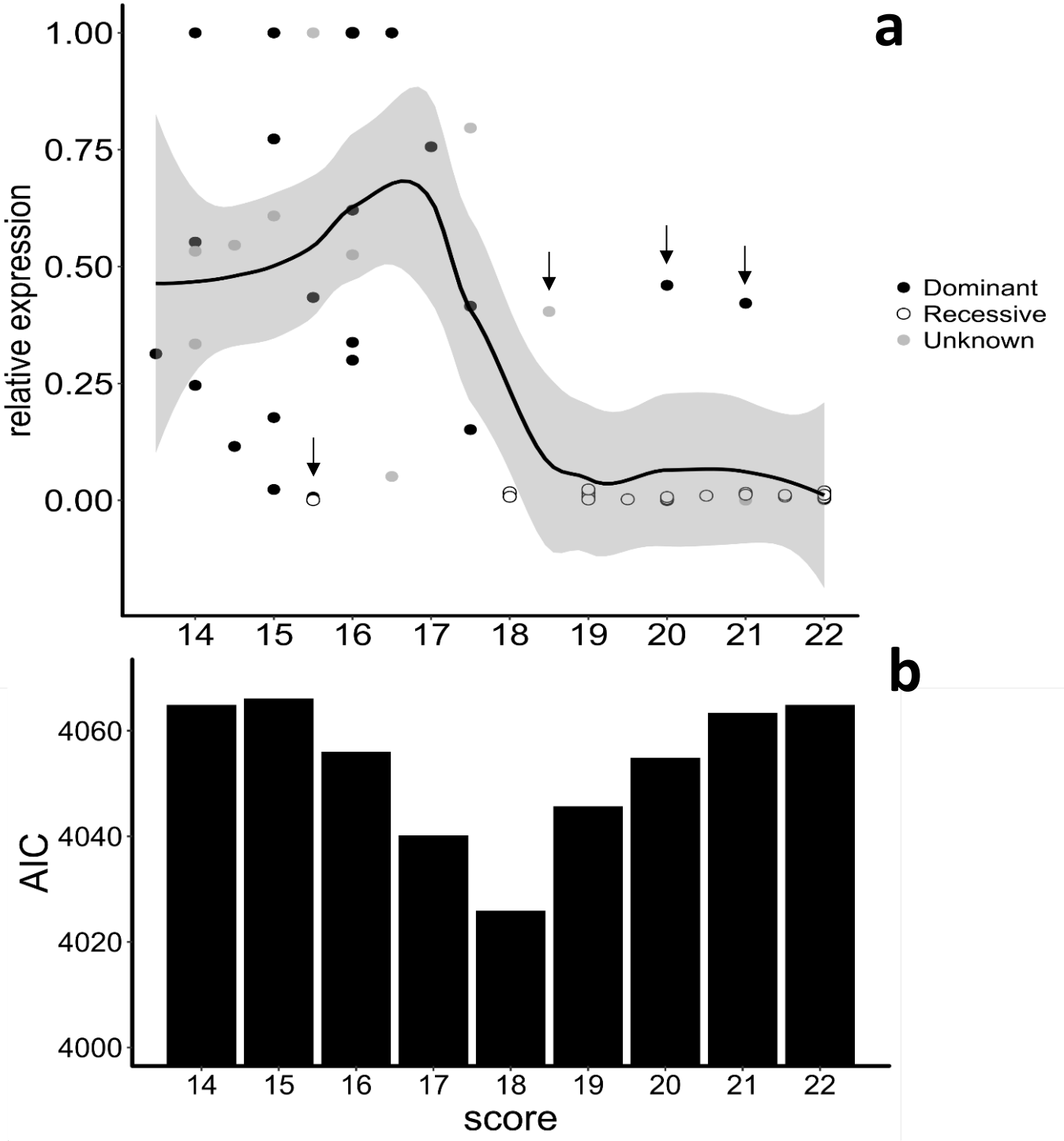

Figure 5

a

```
Ah03 MirS3    3' UACAAGUUCCAUUAUAUAAUCGAA 5'
                 ||||||||||||||x||x|||o||
Ah29 target   5' ATGTTCAAGGTAATTTACTAGTTT 3'
Score = 18.5


Ah04 Mir4239  3' CCUCGUACACCUUUAUUGCCUUUG 5'
                 |||x|||||||x||||||||||||
Ah20 target   5' GGAACATGTGGCAATAACGGAAAC 3'
Score = 20


Ah10 Mir4239  3' CCUCGUACACCUUUAUUGCCUUUGU 5'
                 |||x|||||||x|||||||||||||
Ah20 target   5' GGAACATGTGGCAATAACGGAAACA 3'
Score = 21
```

b

```
Ah04 MirS4    3' GUAUGAUUCUUGUUAGAUUCA 5'
                 ~~~||||||||o||||||||~
Ah03 target   5' ACTACTAAGAATAATCTAAGA 3'
Score = 15,5
```

Figure S1

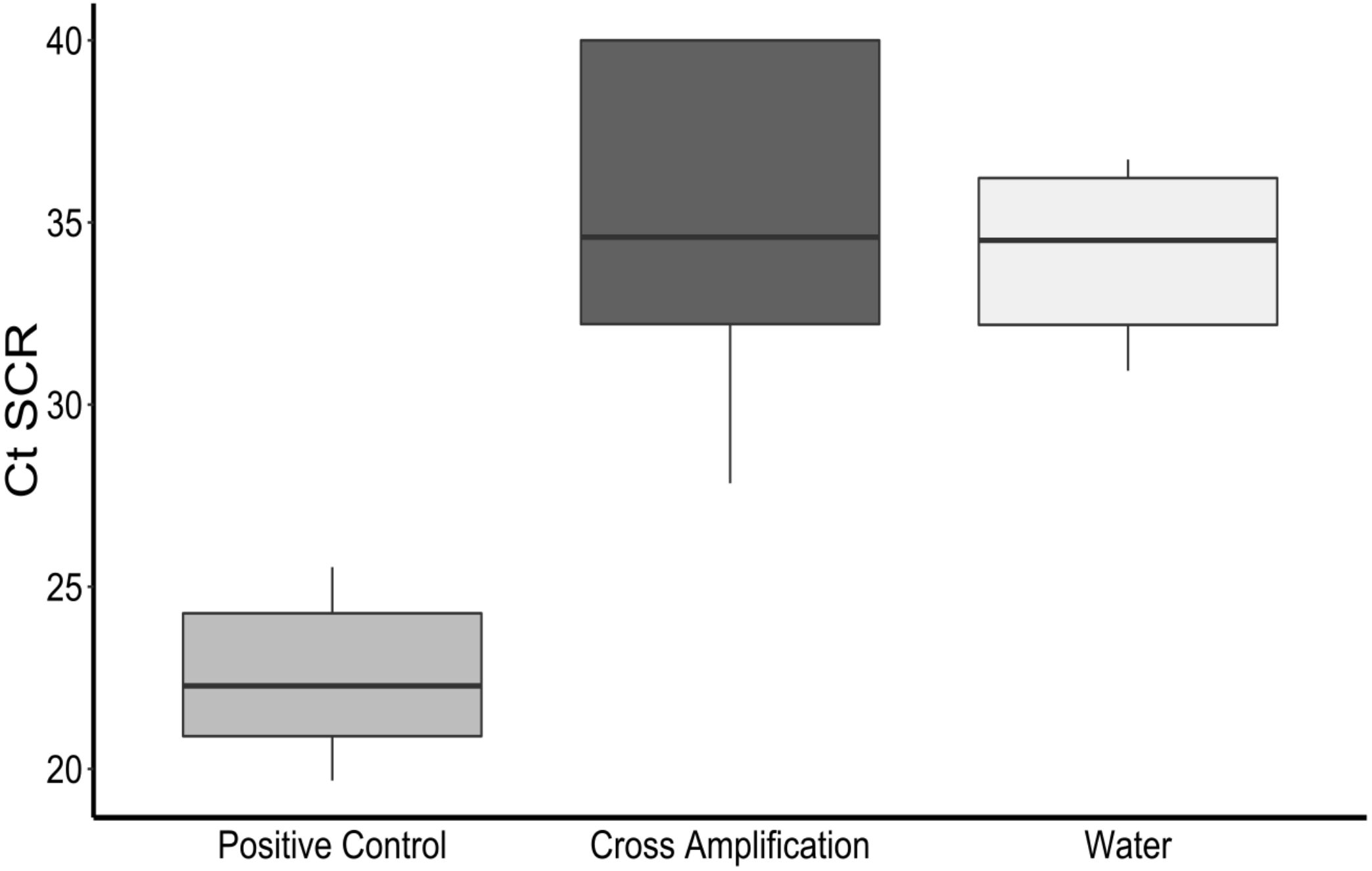

Figure S2

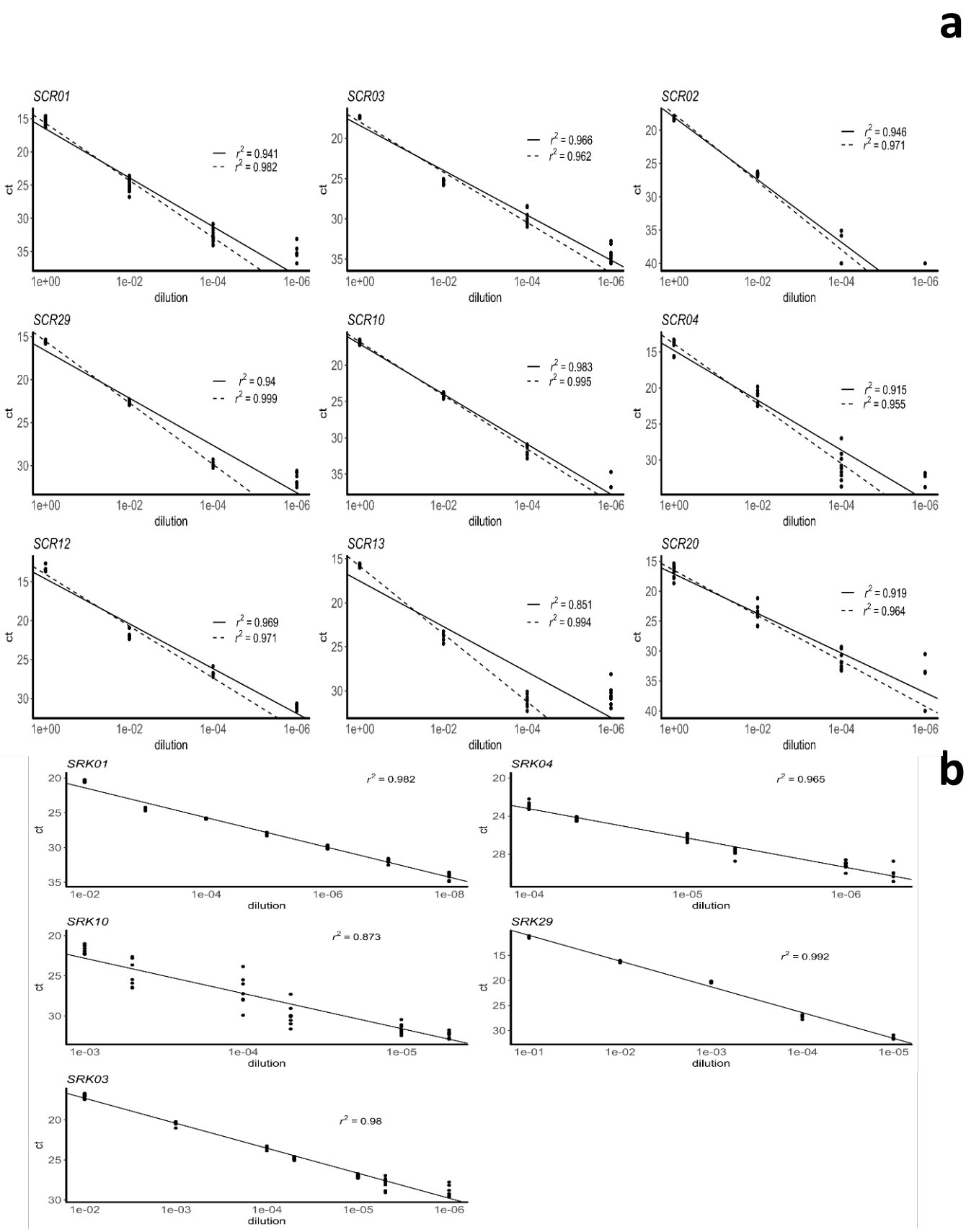

Figure S3

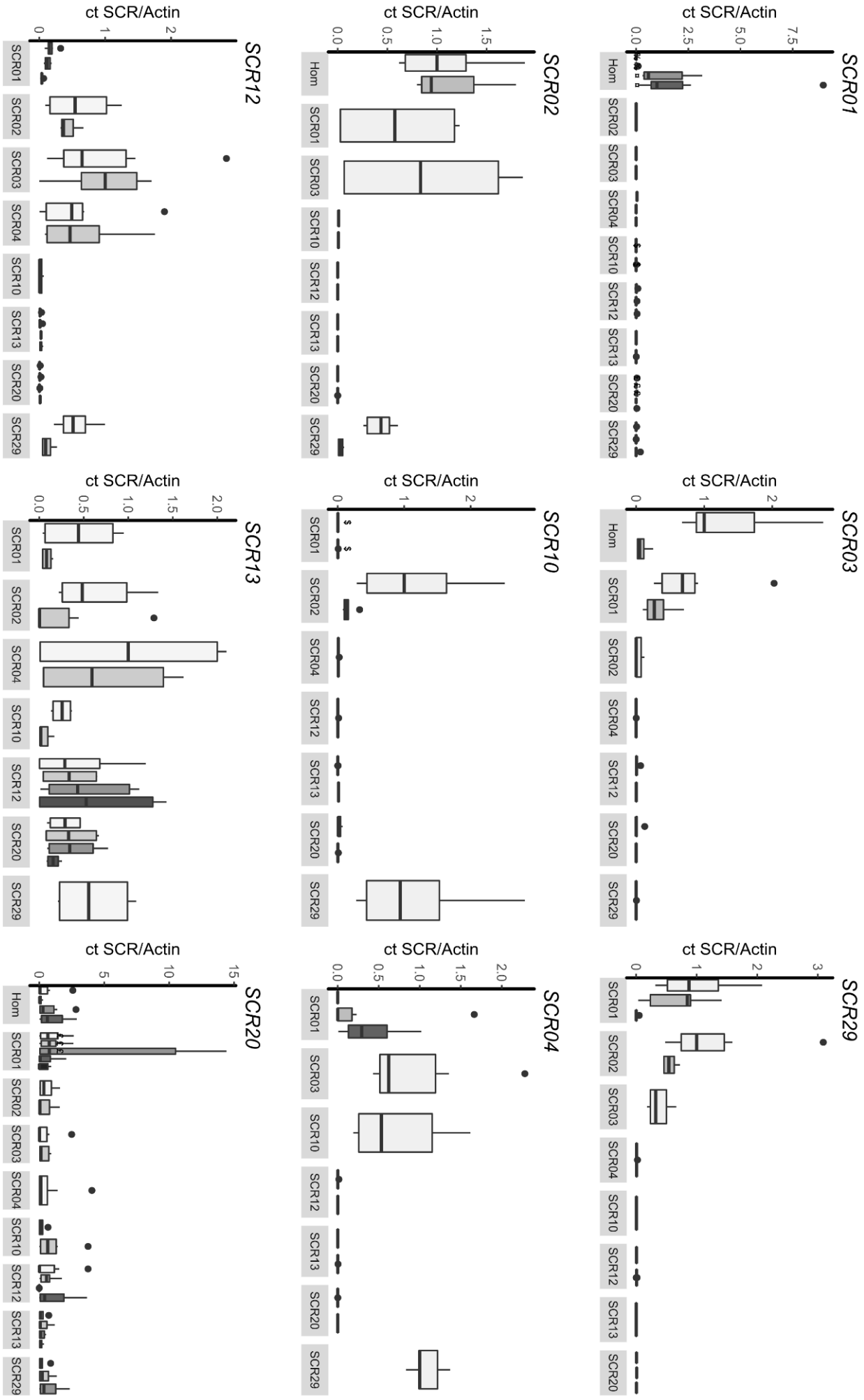

Figure S4


```
lmer(log(s1$Ct_SCR.actine) ~ (1|allele_measured:stage)
+stage*dom_phenotype+
(1|replicatBiol_genotype/replicat_Techclone), na.action=na.omit)
```

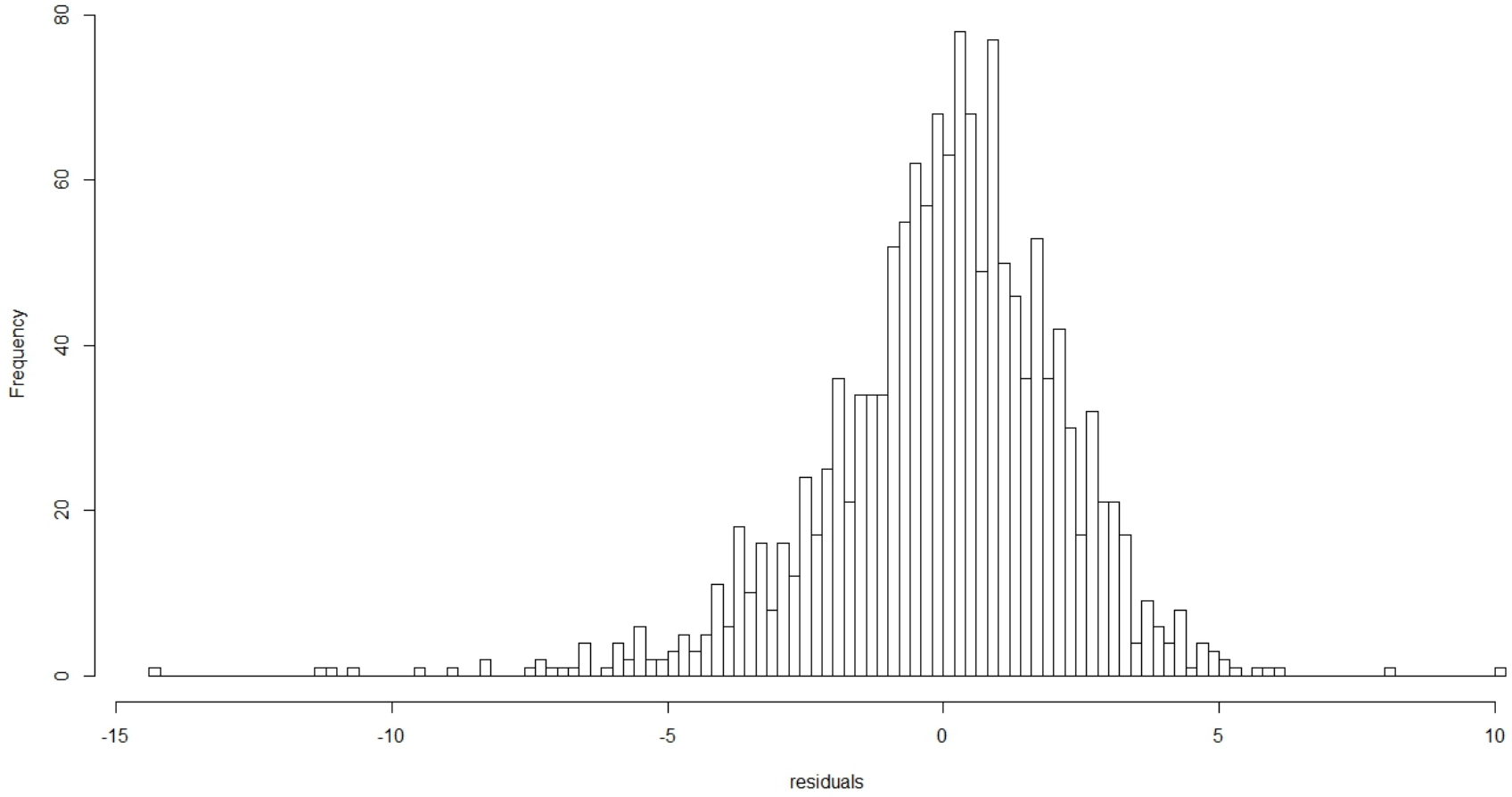

Table S1. SCR samples analysed for each S-locus genotype, showing the number of biological and clone replicates over the four developmental stages sampled. "Allele 1" refers to the first allele noted in the genotype (for example in the S1S2 genotype, "allele 1" is S1 and "allele 2" is S2).

	number of biological replicates	number of expression measure		
		allele 1	allele 2	actin
S1S1	2$	48	48	48
S1S2	1	12	12	12
S1S3	2	24	24	24
S1S4	3	36	36	36
S1S10	1$	24	24	24
S1S12	3	36	36	36
S1S13	2	24	24	24
S1S20	3£	60	60	60
S1S29	3	36	36	36
S2S2	2	24	24	24
S2S3*	2	18	18	18
S2S10	2	24	24	24
S2S12	2	24	24	24
S2S13	2	24	24	24
S2S20	2	24	24	24
S2S29	2	24	24	24
S3S3	2	24	24	24
S3S4	1	12	12	12
S3S12	2	24	24	24
S3S20*	3	30	30	30
S3S29	1	12	12	12
S4S10	1	12	12	12
S4S12	2	24	24	24
S4S13	2	24	24	24
S4S20	2	24	24	24
S4S29	1	12	12	12
S10S12	1	12	12	12
S10S13	2	24	24	24
S10S20	2	24	24	24
S10S29	1	12	12	12
S12S13	4	48	48	48
S12S20	4	48	48	48
S12S29	2	24	24	24
S13S20	4	48	48	48
S13S29	1	12	12	12
S20S20	4	48	48	48
S20S29	3	36	36	36

*: only the stages C and D were sampled for one of the biological replicates

$: two clone replicates per biological replicate

£: two of the three biological replicates are represented by two clone replicates

Table S2: SRK samples analysed for each S-locus genotype, showing the number of biological and clone replicates over the four developmental stages sampled. The alleles are named accordingly to the Table S1.

	number of expression measure		
	allele 1	allele 2	actin
S1S1	12	-	11
S1S2	10	-	12
S1S3	11	-	12
S1S10	9	12	11
S1S12	11	12	12
S1S13	11	-	12
S1S20	8	-	9
S1S29	10	-	9
S3S3	12	-	12
S3S4	8	-	12
S3S12	12	11	12
S3S20	12	-	12
S3S29	12	12	12
S4S10	12	12	12
S4S12	12	9	9
S4S13	8	-	12
S4S29	12	11	12
S10S2	12	-	12
S10S12	11	-	12
S10S13	12	-	12
S10S20	12	-	12
S10S29	12	12	12
S12S20	12	-	12
S12S29	11	12	12
S29S2	12	-	12

Table S3: Dominance relationships between alleles from the different genotypes included in this study as determined by controlled crosses.

pollen genotype	pistil phenotype	number of compatible crosses	dominance phenotype in pollen	reference	dominance phenotype in pistil	reference
S1S1	-	-	-	Durand et al. 2014	-	-
S1S2	[S1]	-	S2>S1	Llaurens et al. 2008	S2>S1	Llaurens et al. 2008
S1S2	[S2]	-		Llaurens et al. 2008		
S1S3	[S1]	-	S3>S1	Durand et al. 2014	-	-
S1S3	[S3]	-		Durand et al. 2014		-
S1S4	[S1]	-	S4>S1	Durand et al. 2014	S4>S1	Llaurens et al. 2008
S1S4	[S4]	-		Durand et al. 2014		
S1S10	[S1]	-	NA	-	-	-
S1S10	[S10]			-		-
S1S12	[S1]	-	S12>S1	Durand et al. 2014	S12>S1	Llaurens et al. 2008
S1S12	[S12]	-		Durand et al. 2014		
S1S13	[S1]	-	S13>S1	Durand et al. 2014	-	-
S1S13	[S13]	-		Durand et al. 2014		-
S1S20	[S1]	-	S20>S1	Durand et al. 2014	S20>S1	Llaurens et al. 2008
S1S20	[S20]	-		Durand et al. 2014		
S1S29	[S1]	-	NA	-	-	-
S1S29	[S29]			-		-
S2S3	[S2]	-	NA	-	-	-
S2S3	[S3]	-		-		-
S2S4	[S2]	-	S4>S2	Llaurens et al. 2008	S4>S2	Llaurens et al. 2008
S2S4	[S4]	-		Llaurens et al. 2008		
S2S10	[S2]	-	NA	-	-	-
S2S10	[S10]	-		-		-
S2S12	[S2]	-	S12>S2	Llaurens et al. 2008	S12>S2	Llaurens et al. 2008
S2S12	[S12]	-		Llaurens et al. 2008		
S2S13	[S2]	-	NA	-	-	-
S2S13	[S13]	-		-		-
S2S20	[S2]	-	NA	-	-	-
S2S20	[S20]	-		-		-
S2S29	[S2]	0/5	S2>S29	This study	-	-
S2S29	[S29]	4/7		This study		-
S3S4	[S3]	-	S4>S3	Durand et al. 2014	-	-
S3S4	[S4]	-		Durand et al. 2014		-
S3S10	[S3]	-	S10>S3	Durand et al. 2014	-	-
S3S10	[S10]	-		Durand et al. 2014		-
S3S12	[S3]	-	S12>S3	Durand et al. 2014	-	-
S3S12	[S12]	-		Durand et al. 2014		-
S3S13	[S3]	-	S13>S3	Durand et al. 2014	-	-
S3S13	[S13]	-		Durand et al. 2014		-
S3S20	[S3]	-	S20>S3	Durand et al. 2014	-	-
S3S20	[S20]	-		Durand et al. 2014		-
S3S29	[S3]	-	S29>S3	-	-	-
S3S29	[S29]	-		-		-
S4S10	[S4]	-	S4>S10	Durand et al. 2014	-	-
S4S10	[S10]	-		Durand et al. 2014		-
S4S12	[S4]	-	S12>S4	Durand et al. 2014	S12>S4	Llaurens et al. 2008
S4S12	[S12]	-		Durand et al. 2014		
S4S13	[S4]	-	S13>S4	Durand et al. 2014	-	-
S4S13	[S13]	-		Durand et al. 2014		-
S4S20	[S4]	-	S20>S4	Durand et al. 2014	S20>S4	Llaurens et al. 2008
S4S20	[S20]	-		Durand et al. 2014		

S4S29	[S4]	-	S4>S29	Durand et al. 2014	-	-
S4S29	[S29]	-		Durand et al. 2014		-
S10S12	[S10]	5/5	S12>S10	This study	-	-
S10S12	[S12]	0/5		This study		-
S10S13	[S10]	-	S13>S10	Durand et al. 2014	-	-
S10S13	[S13]	-		Durand et al. 2014		-
S10S20	[S10]	-	S20>S10	Durand et al. 2014	-	-
S10S20	[S20]	-		Durand et al. 2014		-
S10S29	[S10]	1/5	S10>S29	This study	-	-
S10S29	[S29]	3/3		This study		-
S12S13	[S12]	-	S13>S12	Durand et al. 2014	-	-
S12S13	[S13]	-		Durand et al. 2014		-
S12S20	[S12]	-	S20>S12	Durand et al. 2014	S20>S12	Llaurens et al. 2008
S12S20	[S20]	-		Durand et al. 2014		
S12S29	[S12]	-	S12>S29	Durand et al. 2014	-	-
S12S29	[S29]	-		Durand et al. 2014		-
S13S20	[S13]	-	S13=S20	Durand et al. 2014	-	-
S13S20	[S20]	-		Durand et al. 2014		-
S13S29	[S13]	-	S13>S29	Durand et al. 2014	-	-
S13S29	[S29]	-		Durand et al. 2014		-
S20S29	[S20]	-	S20>S29	Durand et al. 2014	-	-
S20S29	[S29]	-		Durand et al. 2014		-

Table S4: qPCR primer sequences for each *SCR* and *SRK* alleles studied.

		5' Primer Sequence 3'
SCR01	F	AAGTGGAAGCTTGGACGAGA
	R	AAAAGTCGTATCTGCGATTG
SCR02	F	GTCTTTCCTTATAAGCCATGG
	R	GGGGACCCAAGAGATTATGC
SCR03	F	CACATAAAAGAATCATGAAGTCTGC
	R	AATGACAGTGGCAAAGTCGC
SCR04	F	GACGTGTTGTTTTGTTCATGGG
	R	GGCGAGAGGGTCTGAAATTC
SCR10	F	CTCATTGTTTTCTTCACAAGCC
	R	GCGAATGTAAAGATGTTGATGGGG
SCR12	F	CGCTTGTTTTGTGTCACG
	R	GCTTTTAACAGAAACCAGGG
SCR13	F	AGACGTGCTACATTGTTCATAGT
	R	GAGACGGAAACTACAACTGCA
SCR20	F	GACATAGAAGTTCAGAAGGCGC
	R	TGCCGCTGTCAAGTTAATAGAG
SCR29	F	CATGTCTTTGCTTATAAGCC
	R	GCTGGTCGTCGATATTGCCG
SRK01	F	TCAGATTGGCGGCTTCTGAG
	R	TGGAAACAGAAGCAAGCAAGG
SRK03	F	AGGAATGTGAGGAGAGGTGC
	R	GGGCAACAACAACAGTAGGA
SRK04	F	CGGAGAGTTTCGAGATATCCG
	R	GGGTGGTAATGTCAAGTGGG
SRK10	F	ACTTGGGCTGGAAGAATGTG
	R	AGGAAACACAAGCGAGCAAG
SRK12	F	ATGGATGCGATTGTGGACAG
	R	CATTGGTTTGGTAGTTGGAATCA
SRK29	F	CCGAAATTATGCTGCCGATGG
	R	CTTGTGAGTTTCATCATGTACTGGT

Table S5: Detailed results from the generalized linear mixed models.

a. Decomposition of the sources of variance across allele identity and the hierarchical levels biological, clones and technical replicates for *SCR*.

`lmer(log(Ct_SCR.actine) ~ stage*dom_sRNA_prediction+(1|allele_measured:stage)+(1|replicatBiol_genotype)+(1|replicat_Techclone), na.action=na.omit)`

Random effects:	Groups	Name	Variance	Std.Dev.
	replicat_Techclone	(Intercept)	0.4091	0.6396
	replicatBiol_genotype	(Intercept)	1.0795	1.0390
	allele_measured:stage	(Intercept)	4.5674	2.1372
	Residual (Technical replicates)		6.0815	2.4461

---

b. Test of the variation of expression dynamic across *SCR* alleles.

`model 1: lmer(log(Ct_SCR.actine) ~ stage*dom_phenotype+(1|replicatBiol_genotype/replicat_Techclone))`
`model 2 : lmer(log(Ct_SCR.actine) ~ stage*dom_phenotype+(1|allele_measured:stage)+(1|replicatBiol_genotype/replicat_Techclone), na.action=na.omit)`

	Df	AIC	BIC	logLik	deviance	Chisq Chi	Df	Pr(>Chisq)	
model 1:	11	6946.0	7004	-3462.0	6924.0				
model 2:	12	6730.6	6794	-3353.3	6706.6	217.32	1	< 2.2e-16	***

---

c. Test of the dominance and stage effects on *SCR* transcript levels, showing a significant interaction.

`lmer(log(Ct_SCR.actine)~(1|allele_measured:stage)+stade*dom_phenotype+(1|replicatBiol_genotype/replicat_Techclone), na.action=na.omit`

	Sum Sq	Mean Sq	NumDF	DenDF	F.value	Pr(>F)	
stade	213.51	71.17	3	27.53	13.805	1.107e-05	***
dom_phenotype	814.70	814.70	1	302.35	158.025	< 2.2e-16	***
stade:dom_phenotype	596.73	198.91	3	1358.37	38.582	< 2.2e-16	***

---

d. Comparison of the fit of the model under different base-pairing score thresholds.

`lmer(log(Ct_SCR.actine) ~ (1|allele_measured:stage)+stage+Dom_score_based_xx+(1|replicatBiol_genotype/replicat_Techclone) , na.action=na.omit)`

	Df	AIC	BIC	logLik	deviance	Chisq	Df	Pr(>Chisq)	
Dom_score_based_14	23	4064.9	4175.5	-2009.5	4018.9				
Dom_score_based_15	24	4066.1	4181.5	-2009.0	4018.1	0.8294	1	0.3624	
Dom_score_based_16	24	4056.0	4171.5	-2004.0	4008.0	10.0691	0	<2e-16	***
Dom_score_based_17	24	4040.2	4155.6	-1996.1	3992.2	15.8111	0	<2e-16	***
Dom_score_based_18	24	4025.9	4141.3	-1988.9	3977.9	14.3695	0	<2e-16	***
Dom_score_based_19	24	4045.7	4161.1	-1998.9	3997.7	0.0000	0	1.0000	
Dom_score_based_20	24	4054.9	4170.3	-2003.5	4006.9	0.0000	0	1.0000	
Dom_score_based_21	24	4063.4	4178.8	-2007.7	4015.4	0.0000	0	1.0000	
Dom_score_based_22	24	4064.9	4180.3	-2008.5	4016.9	0.0000	0	1.0000	

---

e. Test of the effect of the position of the target on the strength of silencing.

`lmer(log(Ct_SCR.actine)~allele_measured:stage+stage+position_target+(1|allele_measured/replicatBiol_genotype/replicat_Techclone), na.action=na.omit)`

	Sum Sq	Mean Sq	NumDF	DenDF	F.value	Pr(>F)
position_target	27.019	6.755	4	33.275	1.4432	0.241609

---

f. Decomposition of the source of variance across the technical replicates and the allele identity for *SRK*.

```
lmer(log(Ct_SRK.actine) ~ stade*dom_phenotype+(1|allele_measured:stade)+(1|replicat_Techclone), na.action=na.omit)
```

Random effects:	Groups	Name	Variance	Std.Dev.
	allele_measured:stade	(Intercept)	3.1451	1.7734
	replicat_Techclone	(Intercept)	0.6974	0.8351
	Residual		0.8089	0.8994

---

g. Test of the variation of expression dynamic across *SRK* alleles.

```
model 1 :lmer(log(Ct_SRK.actine) ~ stade*dom_phenotype+(1|replicatBiol_genotype/replicat_Techclone) , na.action=na.omit)
model 2 :lmer(log(Ct_SRK.actine) ~ (1|allele_measured:stade)+stade*dom_phenotype+(1|replicatBiol_genotype/replicat_Techclone), na.action=na.omit)
```

	Df	AIC	BIC	logLik	deviance	Chisq Chi	Df	Pr(>Chisq)	
model 1:	11	280.74	307.07	-129.37	258.74				
model 2:	12	275.82	304.56	-125.91	251.82	6.9103	1	0.00857	**

---

h. Test of the effect of stage and dominance on *SRK* transcript levels.

```
lmer(log(Ct_SRK.actine) ~ (1|allele_measured:stade)+stade*dom_phenotype+(1|replicatBiol_genotype/replicat_Techclone), na.action=na.omit)
```

	Sum Sq	Mean Sq	NumDF	DenDF	F.value	Pr(>F)	
stade	2.0520	0.6840	3	3.346	0.8456	0.546472	
dom_phenotype	5.5723	5.5723	1	3.442	6.8884	0.068244	.
stade:dom_phenotype	10.7038	3.5679	3	64.867	4.4107	0.006943	**

---

i. Test of the effect of the identity of the companion allele on *SCR* transcript levels.

```
lmer(log(Ct_SCR.actine) ~ (1|allele_measured:stade)+stage+Other_allele_inGenot+(1|replicatBiol_genotype/replicat_Techclone) , na.action=na.omit)
```

	Sum Sq	Mean Sq	NumDF	DenDF	F.value	Pr(>F)	
Other_allele_inGenot	52.061	10.412	5	32.843	2.2217	0.07558	.

---

j: Test of the effect of age on alignment score above the threshold of 18.

```
lm(score ~ age)
```

	Df	Sum Sq	Mean Sq	F value	Pr(>F)
age	1	0.066	0.06586	0.0362	0.8504
Residuals	29	52.708	1.81753		

Table S6: sRNA and target identified as the best match for every pair of alleles for SCR. CtSCR/Ctactin ratios are given for the target allele in the interaction, calculated from the mean of CtSCR/Ctactin ratios across the two earliest developmental stages (buds below 1mm, see Figure 1). The positions of the targets are given relative to the beginning of the closest exon of SCR for targets upstream from the gene or in the intron), and relative to the stop codon for downstream targets. R: Recessive; D: dominant; H: homozygote.

targeting allele	targeting sRNA precursor	targeted allele	dominance phenotype		Best predicted sRNA/target interaction		score	CtSCR /Ctactin	target location	relative target position	
										from	to
Ah01	Ah01_Mir4239			sRNA 3'	AAAAUAAAAGCAAAAACGACGUA	5'					
					~~||||||--|||||x||||||		14				
		Ah01	H	target 5'	TATTATTTT--TTTTTACTGCAT	3'		1.1342E-02	promotor	-598	-581
	Ah01_Mir4239			sRNA 3'	AAAAU-AAAAGCAAAAACGAC-GUA	5'					
					~~||-|||||-||||||o||-||~		13.5				
		Ah02	D	target 5'	UAUUAUUUUUC-UUUUUGUUGUCAA	3'		1.3053E-01	intron	-196	-177
	Ah01_Mir4239			sRNA 3'	AAAAUA-AAAGCAAAAAC-GACGUA	5'					
					||||-|-|||||||||-||~~~~		15				
		Ah03	D	target 5'	UUUU-UCUUUCGUUUUUGUCUAUUU	3'		2.8473E-02	promotor	-505	-486
	Ah01_Mir4239			sRNA 3'	AAAUAAAAGCAAA-A-ACGACGUAC-UA	5'					
					||||x||||-|||-|-|-||-||||-||		14				
		Ah04	D	target 5'	UUUACUUUC-UUUAUAU-CU-CAUGUAU	3'		1.2298E-01	promotor	-517	-493
	Ah01_Mir4239			sRNA 3'	AGCAAAAACG-A-CGUAC-UAGGU--UCC	5'					
					||x|||||||-|-|o|||-|||||--|||		15.5				
		Ah10	D	target 5'	UCAUUUUUGCAUCGUAUGUAUCCAUCAGG	3'		2.8487E-04	exon	103	131
	Ah01_Mir4239			sRNA 3'	AAAAUAAA-AGCAAA-AA-CGACGUA	5'			2		
					||||||||-|x||||-||-|o|-|||		14.5				
		Ah12	D	target 5'	UUUUAUUUGUAGUUUAUUAGUU-CAU	3'		2.1209E-02	downstream	530	554
	Ah01_Mir4239			sRNA 3'	AG-CAAAAACGACGUACUAGGUUCC	5'					
					||-|||||||||x|o||---|||||		13.5				
		Ah13	D	target 5'	UCUGUUUUUGCUACGUG---CAAGG	3'		2.0399E-02	downstream	1940	1961
	Ah01_Mir4239			sRNA 3'	UCGUACGCCGUUUUUGCCUAUGUU	5'					
					~~||||o|||||x||||||x||||		16.5				
		Ah20	D	target 5'	CACAUGUGGCAAUAACGGAAACAA	3'		2.0770E-01	exon	55	76
	Ah01_Mir4239			sRNA 3'	AGCAAAAACGACGUACUA-GGUUCC	5'					
					~~|||||x||||||-||-|||||~		15				
		Ah29	D	target 5'	UUUUUUUUUCUGCAU-AUGCCAAGA	3'		4.9834E-02	downstream	910	929
Ah02	Ah02_Mir1887			sRNA 3'	GUGAAUCUAACAAGAAUCAUACUC	5'					
					~~|||||||||||||||x|||||~		19				
		Ah01	R	target 5'	CUCUUAGAUUGUUCUUACUAUGAA	3'		5.4584E-05	promotor	-59	-39
	Ah02_MirS3			sRNA 3'	AACUAACCAAUGAGCAUUUU-CA	5'					
					||||||x|x|||-|||||||-||		15				
		Ah02	H	target 5'	UUGAUUUGCUAC-CGUAAAACGU	3'		2.3912E-01	upstream	-1545	-1524
	Ah02_Mir1887			sRNA 3'	GUGAAUCUAACAAGAAUCAUACUC	5'					
					~~|||||||x|||||||o|x||		16.5				
		Ah03	R	target 5'	CUCUUAGAUUAUUCUUAGUGUAAG	3'		1.8790E-03	promotor	-108	-87

	Ah02_MirS3			sRNA	3'	AACUAACCAAUGAGCAUUUUCA	5'						
						|||||||||||x|--||||~~		14					
		Ah04	D	target	5'	UUGAUUGGUUACAC--AAAAAA	3'		Na	intron	-60	-43	
	Ah02_MirS3			sRNA	3'	AACUAACCAAUGAG-CAUUUUCA	5'						
						|||||||||||o-|-|||~~		15.5					
		Ah10	D	target	5'	UUGAUUGGUUACUUAG-AAAACU	3'		4.1045E-02	intron	-56	-37	
	Ah02_MirS3			sRNA	3'	UUUAA-ACG-CUUAUU-GGUUAGUGU	5'						
						|||||-|x|-||||||-|||||||~~		16					
		Ah12	D	target	5'	AAAUUAUUCAGAAUAAGCCAAUCAGA	3'		9.6584E-02	intron	-601	-578	
	Ah02_Mir1887			sRNA	3'	GUGAAUCUAA-CA-AGAAUCAUACUC	5'						
						~||||-||||-||-|||||||~~~~~		14					
		Ah13	D	target	5'	AACUU-GAUUAGUAUCUUAGUCACAA	3'		3.4676E-02	downstream	203	221	
	Ah02_MirS3			sRNA	3'	UUUAAA-CGCUUAU-U--G-GUUAGUGU	5'						
						||||||-||x||||-|--|-||||||~~		14					
		Ah20	D	target	5'	AAAUUUAGCCAAUAUAUGCUCAAUCAAA	3'		6.9471E-02	downstream	1611	1636	
	Ah02_Mir1887			sRNA	3'	GUGAAUCUAACAAGAAUCAUACUC	5'						
						|o||||||x||||||||o|~~~		16					
		Ah29	R	target	5'	CGCUUAGAUAGUUCUUAGUGUAAU	3'		8.1926E-02	promotor	-53	-33	
Ah03	Ah03_MirS3			sRNA	3'	UACAAGUUCCAUUAUAUAAUCGAA	5'						
						||||||||||||||||x|||||		22					
		Ah01	R	target	5'	AUGUUCAAGGUAAUAUAUGAGCUU	3'		4.2927E-05	exon	59	82	
	Ah03_MirS3			sRNA	3'	AGUUCCAUUAUAUAAUC-GAAGAAA	5'						
						|||||||||x||x|||-o||||||		17.5					
		Ah02	D	target	5'	UCAAGGUAAUUUACUAGUUUUCUUU	3'		1.9047E-01	intron-exon boundary	-19	5	
	Ah03_MirS5			sRNA	3'	AUACGAAAGUACAGA--AAAAAAAG	5'						
						||||o||||||||-|--|||||||~		16.5					
		Ah03	H	target	5'	UAUGUUUUCAUGU-UGGUUUUUUUA	3'		3.6834E-02	exon	-21	1	
	Ah03_MirS3			sRNA	3'	ACA-AGUU-CCAUUAUAUAAUCGAAG	5'						
						|||-||||-||-||||||x||-|||~		15					
		Ah04	D	target	5'	UGUGUCAAUGG-AAUAUACUA-CUUU	3'		5.0001E-01	intron	-1221	-1199	
	Ah03_MirS5			sRNA	3'	AAAA-AAG-GUUCAGUACAAUUUC	5'						
						||||-|||-||||x|||x||||||		16					
		Ah10	D	target	5'	UUUUCUUCACAAGCCAUAUUAAAG	3'		Na	exon	84	107	
	Ah03_MirS3			sRNA	3'	ACAAGUUCCAUUAUAUAAUCGAAG	5'						
						||||||||||||-|-x||-||||		16					
		Ah12	D	target	5'	UGUUCAAGGUAAU-U-CUA-CUUC	3'		1.8389E-01	promotor	-569	-549	
	Ah03_Mirs3			sRNA	3'	AGUUCCAUUAUAUAA-U-CGAAGAAA	5'						
						||||||||||||||-|-x|||o|||		18.5					
		Ah13	D	target	5'	UCAAGGUAAUAUAUUAACACUUUUUU	3'		Na	intron-exon boundary	63	88	
	Ah03_MirS5			sRNA	3'	AUACGAAAGUACAGAA-AAA--AAAG	5'						
						|||-||||x|||||||-|||--||||		16					
		Ah20	D	target	5'	UAU-CUUUAAUGUCUUGUUUAAUUUC	3'		6.2263E-02	downstream	1478	1502	

	Ah03_MirS3			sRNA	3'	UACAAGUUCCAUUAUAUAAUCGAA	5'					
						||||||||||||x||x|||o||		18.5				
		Ah29	R	target	5'	AUGUUCAAGGUAAUUUACUAGUUU	3'		3.3086E-02	intron-exon boundary	-8	15
Ah04	Ah04_MirS4			sRNA	3'	UAU-ACUUUUUUC-UUUUUUCU-UU	5'					
						|||-||-||||||-||||||||-||		17				
		Ah01	R	target	5'	AUAUUG-AAAAAGUAAAAAAGAGAA	3'		1.7497E-04	upstream	-1173	-1150
	Ah04_Mir867			sRNA	3'	ACAGAAAGGAUUAUUUGGUACAAGUU	5'					
						|||||||||x||||o|||||x||||		20.5				
		Ah02	R	target	5'	UGUCUUUCCUUAUAAGCCAUGGUCAA	3'		Na	exon	2	27
	Ah04_MirS4			sRNA	3'	GUAUGAUUCUUGUUAGAUUCA	5'					
						~~||||||||o||||||||~		15.5				
		Ah03	R	target	5'	ACUACUAAGAAUAAUCUAAGA	3'		1.8947E-05	intron-exon boundary	-20	3
	Ah04_MirS4			sRNA	3'	AA-AA-GAAAC-AGUAUUGUGAUAAAGA	5'					
						||-||-|||||-||||||o|||||||~~		18.5				
		Ah04	H	target	5'	UUCUUACUUUGAUCAUAAUACUAUUUAU	3'		Na	intron	-2057	-2032
	Ah04_MirS4			sRNA	3'	AUAGGUCUUUGUCGCUAACAAUGA	5'					
						||||||x|||o||o||||||||||		19				
		Ah10	R	target	5'	UAUCCAAAAAUAGUGAUUGUUACU	3'		6.6149E-04	intron	-872	-849
	Ah04_MirS4			sRNA	3'	UAUAC-UUU-UUUC-UUUUUUCUUU	5'					
						~||x|-|||-||||-||||||||||		16				
		Ah12	D	target	5'	UUAAGAAAAGAAAGAAAAAAAGAAA	3'		1.1418E-01	promotor	-273	-250
	Ah04_MirS4			sRNA	3'	UAUACUUUUUU--C-UUUUU--UCUUU	5'					
						~||||||||||--|-|||||--|||||		16				
		Ah13	D	target	5'	UUAUGAAAAAAGUGUAAAAAGUAGAAA	3'		6.5069E-02	downstream	1024	1049
	Ah04_Mir4239_copy1			sRNA	3'	CCUCGUACACCUUUAUUGCCUUUG	5'					
						|||x||||||x||||||||||||		20				
		Ah20	D	target	5'	GGAACAUGUGGCAAUAACGGAAAC	3'		9.5550E-02	exon	51	74
	Ah04_Mir867			sRNA	3'	ACAGAAAGGAUUAUUUGGUACAAGUU	5'					
						|||||||x||x||||o||||||||||		20.5				
		Ah29	R	target	5'	UGUCUUUGCUUAUAAGCCAUGUUCAA	3'		8.0761E-04	exon	40	65
Ah10	Ah10_Mir1887			sRNA	3'	GGAGUAUGAUUCUUGUUAGAUUCA	5'					
						|o||||x|||||||||||||~		19.5				
		Ah01	R	target	5'	CUUCAUAGUAAGAACAAUCUAAGA	3'		2.5148E-05	promotor	-61	-39
	Ah10_Mir867			sRNA	3'	AGAAAGGAAUAUUCGGUACAAGUU	5'					
						|||||||||||||||||x||||		22				
		Ah02	R	target	5'	UCUUUCCUUAUAAGCCAUGGUCAA	3'		2.0406E-03	exon	2	25
	Ah10_Mir1887			sRNA	3'	GGAGUAUGAUUCUUGUUAGAUUCA	5'					
						|||o|x|||||||o||||||||~		18				
		Ah03	R	target	5'	CCUUACACUAAGAAUAAUCUAAGA	3'		Na	promotor	-109	-87
	Ah10_Mir867			sRNA	3'	GCAACUUUUAACAAAUAUUCCU-UU	5'					
						~~||x|||||x|||||||||||-||		17				
		Ah04	R	target	5'	UUUUCAAAAUGGUUUAUAAGGAGAA	3'		3.7813E-01	exon	90	112
	Ah10_Mir4239			sRNA	3'	UUGUUUC-UUACGUUUGUUCUG-GAA	5'					

											14.5				
		Ah10	H	target	5'	AACAAAGAAAUG--AACAA-AUGCUU	3'			Na		dowstream		136	158
	Ah10_Mir867			sRNA	3'	AGAAAGGAAUAUUCGGUACAAGUU	5'								
									15						
		Ah12	D	target	5'	UCUUUCUUU-UAAAUGAUGUUCAA	3'			4.2743E-03		promotor		-555	-533
	Ah10_Mir4239			sRNA	3'	UUGUUUCUUAC-GUUUGUUCUGGAA	5'								
									15						
		Ah13	D	target	5'	AAC-AAGAAUGACGAACACGAUCUC	3'			1.1520E-02		downstream		714	736
	Ah10_Mir4239			sRNA	3'	CCUCGUACACCUUUAUUGCCUUUGU	5'								
									21						
		Ah20	D	target	5'	GGAACAUGUGGCAAUAACGGAAACA	3'			8.7536E-02		exon		51	75
	Ah10_Mir867			sRNA	3'	AGAAAGGAAUAUUCGGUACAAGUU	5'								
									22						
		Ah29	R	target	5'	UCUUUGCUUAUAAGCCAUGUUCAA	3'			4.2462E-04		exon		42	65
Ah12	Ah12_Mirs3			sRNA	3'	UUAGUUUUGGAUUUCCUCCAACUAU	5'								
									21						
		Ah01	R	target	5'	AAUCAAAACCAAAAGGAUGUUGAUA	3'			1.8177E-04		intron		-238	-215
	Ah12_MirS3			sRNA	3'	UUUAGUUUUGGAUUUCCUCCAACUA	5'								
									21						
		Ah02	R	target	5'	AAAUCAAAACCAAAAGGAUGUUGAU	3'			6.0314E-05		intron		-940	-916
	Ah12_MirS3			sRNA	3'	UUAGUUUUGGAUUUCCUCCAACUAU	5'								
									21.5						
		Ah03	R	target	5'	AAUCAAAACUUAAAGGAUGUUGAUA	3'			4.1965E-04		intron		-211	-187
	Ah12_MirS3			sRNA	3'	UUAGUUUUGGA-UUUCCUCCAACUAU	5'								
									20						
		Ah04	R	target	5'	AAUCAAAA-CUAAAAGGACGUUGAUA	3'			1.6505E-03		intron		-79	-55
	Ah12_MirS3			sRNA	3'	UUUAGUUUUGGA-UUUCCUCCAACUA	5'								
									19						
		Ah10	R	target	5'	AAAUCAAAA-CUAAAAGGACGUUGAU	3'			3.2426E-04		intron		-74	-51
	Ah12_MirS3			sRNA	3'	GACGAAAG-AAAAUCGAAACUAAGC	5'								
									15.5						
		Ah12	H	target	5'	UUUCUUUCUUUUUGGCUUUGAUUGG	3'			Na		downstream		123	123
	Ah12_MirS3			sRNA	3'	UUUA-GUUUUGGAUUUCCUCCAACUA	5'								
									14						
		Ah13	D	target	5'	AUAUCCAAAA-AUAAAGGA--UUGAU	3'			3.5946E-02		promotor		-179	-159
	Ah12_MirS3			sRNA	3'	UUUAGUUUUGGA-UUUCC--UCCAACUA	5'								
									15.5						
		Ah20	D	target	5'	AAAUCAAAA-CUAAAAGGAUAUGUUGGU	3'			9.0139E-02		intron		-193	-168
	Ah12_MirS3			sRNA	3'	UUAGUUUUGGA-UUUCCUCCAACUAU	5'								
									20						
		Ah29	R	target	5'	AAUCAAAA-CUGAAAGGACGUUGAUA	3'			5.8038E-04		intron		-225	-201
Ah13	Ah13_MirS3			sRNA	3'	CUCAUUGGUUAGUUUUGGAUUUCCU	5'								
									22						

		Ah01	R	target	5'	AAGUAACCAAUCAAAACCAAAAGGA	3'		6.6402E-05	intron	-231	-208
	Ah13_MirS3			sRNA	3'	UAGUUUUGGAUUUCCUUCAACUAU	5'					
						|||||||||x|||||x|||||||		20				
		Ah02	R	target	5'	AUCAAAACCAAAAGGAUGUUGAUA	3'		7.0608E-05	intron	-938	-915
	Ah13_MirS3			sRNA	3'	UAGUUUUGGAUUUCCUUCAACUAU	5'					
						||||||||o||||||x|||||||		20.5				
		Ah03	R	target	5'	AUCAAAACUUAAAGGAUGUUGAUA	3'		Na	intron	-211	-188
	Ah13_MirS3			sRNA	3'	CUCAUUGGUUAGUUUUGGA-UUUCCU	5'					
						~~||||||||||||||-||-||||||		20				
		Ah04	R	target	5'	GUGUAACCAAUCAAAA-CUAAAAGGA	3'		7.3639E-04	intron	-71	-49
	Ah13_MirS3			sRNA	3'	CU-AAAACGACUCAUUGGUUAGUUUUG	5'					
						||-||||-||x||||||||||||||		21				
		Ah10	R	target	5'	GAGUUUU-CUAAGUAACCAAUCAAAAC	3'		4.9442E-04	intron	-59	-34
	Ah13_MirS2			sRNA	3'	AUAUAUACGCAUUACUGUAUUUGU	5'					
						|||||||||||||||||||||~~		22				
		Ah12	R	target	5'	UAUAUAUGCGUAAUGACAUAAAAA	3'		3.5373E-03	promotor	-470	-449
	Ah13_MirS3			sRNA	3'	AAGAAAA-UCGAA-ACUAACCAAU	5'					
						||-||||-||-||-||||||||~		15				
		Ah13	H	target	5'	UU-UUUUGAG-UUCUGAUUGGUUG	3'		Na	intron	-95	-75
	Ah13_MirS3			sRNA	3'	UUAGUUUUGGA-UUUCCU-U-CAACUA	5'					
						||||||||-||-||||||-|-||||o|		17.5				
		Ah20	D	target	5'	AAUCAAAA-CUAAAAGGAUAUGUUGGU	3'		3.1419E-02	intron	-193	-168
	Ah13_MirS3		D	sRNA	3'	UUUGGA-UUUCCUUCAACUAUAUAU	5'					
						|||x||-||||||x||||||||||		19				
		Ah29	R	target	5'	AAAACUGAAAGGACGUUGAUAUAUA	3'		1.4935E-04	intron	-229	-205
Ah20	Ah20_MirS3			sRNA	3'	AUAGUUGAAGGAAAACCAAAACUAG	5'					
						|||||||x|||||||||||||~		22				
		Ah01	R	target	5'	UAUCAACAUCCUUUUGGUUUUGAUU	3'		1.3491E-04	intron	-239	-216
	Ah20_MirS3			sRNA	3'	AUAGUUGAAGGAAAACCAAAACUAG	5'					
						|||||||x|||||||||||||~		22				
		Ah02	R	target	5'	UAUCAACAUCCUUUUGGUUUUGAUU	3'		1.9359E-05	intron	-938	-915
	Ah20_MirS3			sRNA	3'	AUAGUUGAAGGAAAACCAAAACUAG	5'					
						|||||||x|||||xx||||||||~		18				
		Ah03	R	target	5'	UAUCAACAUCCUUUAAGUUUUGAUU	3'		6.3463E-04	intron	-211	-188
	Ah20_MirS3			sRNA	3'	AUAGUUGAAGGAAAACCAAAACUAG	5'					
						|||||||x|||||||x||||||||~		20				
		Ah04	R	target	5'	UAUCAACGUCCUUUUAGUUUUGAUU	3'		3.0334E-04	intron	-79	-56
	Ah20_MirS3			sRNA	3'	UAGUUGAAGGAAAACCAAAACUAG	5'					
						||||||x|||||||x||||||||~		19				
		Ah10	R	target	5'	AUCAACGUCCUUUUAGUUUUGAUU	3'		9.5621E-04	intron	-74	-52
	Ah20_MirS2			sRNA	3'	CGUCGUAUUGUGCAUUUGUGUAU	5'					
						||||||||||||||||||o||||		21.5				
		Ah12	R	target	5'	GCAGCAUAACACGUAAACGCAUA	3'		1.4779E-03	promotor	-501	-479

	Ah20_MirS2			sRNA	3'	CACAAAUAC-ACAAAUUCACAAUAC	5'								
						||-||||||-|-|||||x|||||~		16							
		Ah13	D	target	5'	GU-UUUAUGAU-UUUAAGCGUUAUU	3'		2.1991E-02		downstream		1322	1343	
	Ah20_MirS3			sRNA	3'	GUUG-A-AGGAAAACCAAAACUAGCC	5'								
						||||-|-||||||x|||||||o|~		17.5							
		Ah20	H	target	5'	CAACAUAUCCUUUUAGUUUUGAUUGU	3'		8.6244E-02		intron		-191	-167	
	Ah20_MirS2			sRNA	3'	CACAAAUACAGAAACACAUAUACA	5'								
						||||||||||x|||-|||||||~~		18							
		Ah29	R	target	5'	GUGUUUAUGUGUUU-UGUAUAUUC	3'		6.2265E-04		promotor		-205	-185	
Brassica S44	S44_Smi2			sRNA	3'	UUCUGUAUGUGCUUAUUUCACACA	5'					-			
						|o||x|x|||||||||o||||||		17							
		S29-pro	R	target	5'	AGGAAACACACGAAUAAGGUGUGU	3'		-		-				
	S44_Smi2			sRNA	3'	UUC-UGUAUGUGCUUAUUUCACACA	5'					-			
						~||-|||x||||x|||||o||||||		16.5							
		S40-pro	R	target	5'	AAGUACACACACAAAUAAGGUGUGU	3'		-		-				
	S44_Smi2			sRNA	3'	UUCUGUAUGUGCUUAUUUCACACA	5'					-			
						~~|||x|||||||||o|||||~		16.5							
		S60-pro	R	target	5'	ACAACACACACGAAUAAGGUGUGA	3'		-		-				
	S44_Smi2			sRNA	3'	UUCUGUAUGUGCUUAUUUCACACA	5'					-			
						|o||o|x||o||||-||||-||||		13.5							
		S44-pro	H	target	5'	AGGAUACACGCGAA-AAAG-GUGU	3'		-		-				
Brassica S60	S60_Smi2			sRNA	3'	UUCUAUAUGUGUUUAUUCCACACA	5'					-			
						|o||x|x|||o||||||||||||									
		S29-pro	R	target	5'	AGGAAACACACGAAUAAGGUGUGU	3'	17	-		-				
	S60_Smi2			sRNA	3'	UUC-UAUAUGUGUUUAUUCCACACA	5'					-			
						~||-|x|x|||||||||||||||		18							
		S40-pro	R	target	5'	AAGUACACACACAAAUAAGGUGUGU	3'		-		-				
	S60_Smi2			sRNA	3'	UUCUAUAUGUGU--UUAUUCCACACA	5'					-			
						~~||x|||||--||||||||||~		15							
		S60-pro	H	target	5'	UACAUACACACACGAAUAAGGUGUGA	3'		-		-				
	S60_Smi2			sRNA	3'	UUCUAUAUGUG-UUUAUUCCACACA	5'					-			
						|o|||x||o|-|||-|||||||~~		14							
		S44-pro	D	target	5'	AGGAUACACGCGAAA-AAGGUGUAU	3'		-		-				
Brassica S40	S40_Smi2			sRNA	3'	UUCUAUAUGUGCUUAUUUCACACA	5'					-			
						|o||x|x||||||||o||||||		17							
		S29-pro	R	target	5'	AGGAAACACACGAAUAAGGUGUGU	3'		-		-				
	S40_Smi2			sRNA	3'	UUC-UAUAUGUGCUUAUUUCACACA	5'					-			
						~||-|x|x||||x|||||o||||||		14.5							
		S40-pro	H	target	5'	AAGUACACACACAAAUAAGGUGUGU	3'		-		-				
	S40_Smi2			sRNA	3'	UUCUAUAUGUGCUUAUUUCACACA	5'					-			
						~~|||||||||o|||||~		14.5							
		S60-pro	D	target	5'	ACACGAAACACGAAUAAGGUGUGA	3'		-		-				

	S40_Smi2			sRNA	3'	UUCUAUAUGUGCUUAUUUCACACA	5'			-				
						|o|||x||o||||-||||-||||		15						
		S44-pro	D	target	5'	AGGAUACACGCGAA-AAAG-GUGU	3'		-	-				
Brassica S29	S29_Smi2			sRNA	3'	UUCUAUAUGUGCUUAUUGCACACA	5'			-				
						|o||x|x|||||||||x||||||								
		S29-pro	H	target	5'	AGGAAACACACGAAUAAGGUGUGU	3'	16.5	-	-				
	S29_Smi2			sRNA	3'	UUC-UAUAUGUGCUUAUUGCACACA	5'			-				
						~||-|x|x|||x||||x|||||								
		S40-pro	D	target	5'	AAGUACACACACAAAUAAGGUGUGU	3'	14	-	-				
	S29_Smi2			sRNA	3'	UUCUAUAUGUGCUUAUUGCACACA	5'			-				
						~~|||||||||x||||~								
		S60-pro	D	target	5'	ACACGAAACACGAAUAAGGUGUGA	3'	14	-	-				
	S29_Smi2			sRNA	3'	UUCUAUAUGUGCUUAUUGCACACA	5'			-				
						|o|||x||o|||x||x||||~~								
		S44-pro	D	target	5'	AGGAUACACGCGAAAAAGGUGUAU	3'	13	-	-				
Brassica S9	S9-Smi			sRNA	3'	ACAUUGAUAAAAUGUGCAUUUGUA	5'							-
						~~||||||x|||||||||||		17						
		S29-SP11	R	target	5'	CUAUUCUAUUUCACACGUAAACAU	3'			-				-
	S9-Smi			sRNA	3'	ACAUUGAUAAAAUGUGCAUUUGUA	5'							-
						~~||||||x|||||||||||		17						
		S40-SP11	R	target	5'	CUAUUCUAUUUCACACGUAAACAU	3'			-				-
	S9-Smi			sRNA	3'	ACAUUGAUAAAAUGUGCAUUUGUA	5'							-
						~~|||||||||||||||||~		18						
		S60-SP11	R	target	5'	CUAUUCUAUUUUACACGUAAACAA	3'			-				-
	S9-Smi			sRNA	3'	ACAUUGAUAAAAUGUGCAUUUGUA	5'							-
						~~||||||x|||||||||||		17						
		S44-SP11	R	target	5'	CUAUUCUAUUUCACACGUAAACAU	3'			-				-
Brassica S60	S60-smi			sRNA		ACAUUGAUAAAAUGAGCAUUUGUA	5'							-
						~~||||||x||x||||||||								
		S29-SP11	R	target		CUAUUCUAUUUCACACGUAAACAU	3'	15		-				-
	S60-smi			sRNA		ACAUUGAUAAAAUGAGCAUUUGUA	5'							-
						~~||||||x||x||||||||								
		S40-SP11	R	target		CUAUUCUAUUUCACACGUAAACAU	3'	16		-				-
	S60-smi			sRNA		ACAUUGAUAAAAUGAGCAUUUGUA	5'							-
						~~|||||||||x|||||||~								
		S60-SP11	H	target		CUAUUCUAUUUUACACGUAAACAA	3'	15		-				-
	S60-smi			sRNA		ACAUUGAUAAAAUGAGCAUUUGUA	5'							-
						~~||||||x||x||||||||								
		S44-SP11	D	target		CUAUUCUAUUUCACACGUAAACAU	3'	15		-				-